Title
Patronin Regulates the Microtubule Network by Protecting Microtubule Minus Ends

Author
Goodwin, Sarah

Publication Date
2011

Peer reviewed|Thesis/dissertation

Patronin Regulates the Microtubule Network By Protecting Microtubule Minus Ends

by

Sarah Goodwin

DISSERTATION

Submitted in partial satisfaction of the requirements for the degree of

DOCTOR OF PHILOSOPHY

in

Cell Biology

Acknowledgements

This thesis is dedicated to my parents, who have given me never-ending support and encouragement.

First and foremost, I want to acknowledge my thesis advisor, Ron Vale, who has been an incredible mentor to me. He pushed my science to be the best it could possibly be and helped me grow as a scientist considerably during my time in graduate school. He always supported my interest in science education and outreach and gave me additional outreach opportunities through the iBioSeminar project. Ron has shown me that one can be a great scientist and also make public outreach and education a priority. I am so grateful that I have met such an amazing role model early in my scientific career.

Dave Morgan and Wallace Marshall, members of my thesis committee, gave me great advice and guidance on my project. Dave Morgan has always been very supportive of me and it has been a pleasure to work near him and his laboratory over the last several years. Wallace is one of the most enthusiastic professors I have ever met and I appreciate his ability to always make science fun and exciting. Orion Weiner, Carol Gross, and James Wells also gave me excellent guidance and help on my project.

I would like to thank Eric Griffis, who was an important mentor to me throughout my graduate career. Eric went above and beyond the call of duty to teach me

experiments and discuss my project with me. He is also a great friend, and my time in graduate school would not have been as rich without him there.

Gohta Goshima and Nico Stuurman performed the initial mitotic spindle screen. In the short time we overlapped, Gohta taught me an incredible amount about cell biology. I have also used several of the many reagents he made while in the Vale lab. Nico helped me on a regular basis on the microscopes and I have had numerous useful discussions with him about my project.

Andrew Carter was my rotation advisor and taught me how to do microtubule in vitro assays. The in vitro assays in this thesis would not have been possible without his help and knowledge.

Melissa Hendershott rotated in the Vale lab during the winter of 2011 and helped with an effort to identify Patronin interaction partners. I am very grateful and excited that she is continuing to work on Patronin.

I want to thank Susana Ribeiro, Thomas Huckaba, Sabine Petry, Carol Cho and all the members of the Vale lab for creating a wonderful environment in which to do science. Special thanks to Phoebe Grigg and Nan Zhang for making the lab run smoothly.

I spent an amazing summer with the Physiology Course and Cell Division Group at the Marine Biological Laboratories in Woods Hole, MA. This summer provided me

with invigorating discussions and fantastic friendships. In particular, I want to thank Brad Zuchero, Sabine Petry, Sisi Chen, and Irina Matos, each of whom made the summer extra special.

I want to thank my friends at UCSF, in particular Arthur Millius, Alana Lerner, Cheryl Chun, Mike D'Ambrosio, Chris Brown, Becky Brown, Han Li, Manisha Ray, Paul Temkin, Cecily Burrill, Lisa Watson, Chris Cain, Mari Nishino, Andrew Houk, Ben Engel, Yari Sigal, and Lauren Booth for making graduate school as fun as possible.

Lastly I want to thank my family, Lee, Linda, Amy, and Rachel. I could not have gotten through graduate school without their constant love and support!

Acknowledgement of Published Materials

Part of the text of this thesis is a reprint of the material as it appears in: Goodwin, S.S., and Vale, R.D. (2010). Patronin regulates the microtubule network by protecting microtubule minus ends. Cell *143*, 263-74. The coauthor listed in this publication directed and supervised the research that forms the basis for the thesis.

Patronin Regulates the Microtubule Network by Protecting Microtubule Minus Ends

Sarah Goodwin

Microtubules are the principle scaffold of the mitotic spindle, serve as tracks for intracellular transport of proteins and mRNAs, and also participate in signaling functions. Microtubules are polymers of α/β tubulin heterodimers, which polymerizes in a head-to-tail to form polar filaments. *In vitro* both the plus and minus end of the microtubule undergo dynamic instability, whereby the microtubule undergoes prolonged periods of growth and shrinkage, with infrequent transitions between the two. *In vivo*, the plus end of the microtubule is very dynamic, and many proteins have been identified that bind at microtubule plus ends and regulate dynamicity. However, in contrast to the wealth of information on the microtubule plus end, the regulation of the microtubule minus end *in vivo* is poorly understood. Minus ends are mostly static within the cell, suggesting that microtubule minus ends might be capped by some unknown protein(s) that suppresses subunit dynamics.

In a whole-genome RNAi screen for spindle morphology defects in Drosophila S2 cells, I identified a previously uncharacterized protein whose depletion caused short spindles in mitosis and microtubule fragments in interphase. This protein, which we have named Patronin for the Latin 'patronus' (protector), protects microtubule minus ends *in vivo* from depolymerization by Kinesin-13. In the absence of Patronin, microtubules release from their nucleating sites and treadmill through the cytoplasm, a result of unhindered minus end depolymerization. Purified Patronin selectively binds to and protects minus ends from Kinesin-13-induced depolymerization *in vitro*, demonstrating

that Patronin alone is sufficient to confer minus end stability. Thus, Patronin is the first protein shown to cap and stabilize the microtubule minus end *in vivo*. Furthermore, we demonstrate that microtubule minus end dynamics are regulated by competing actions of destabilizing and stabilizing proteins, as has been shown previously for the plus end. We also identify Patronin interaction partners and provide evidence suggesting that Patronin may be involved in scaffolding centrosomal proteins at microtubule nucleation sites throughout the cytoplasm.

Table of Contents

List of Tables

Chapter 1

List of Figures

Chapter 1

Chapter 2

Introduction

Microtubules are the principle scaffold of the mitotic spindle, serve as tracks for intracellular transport of proteins and mRNAs, and also participate in signaling functions. The repeating subunit of the microtubule is the α/β tubulin heterodimer, which polymerizes in a head-to-tail fashion to form protofilaments; typically ~13 protofilaments associate laterally to form the microtubules seen *in vivo*. Due to the head-to-tail assembly, the microtubule is a polar filament, with β-tubulin facing the plus end and α-tubulin at the minus end (Mitchison, 1993). *In vitro* experiments using purified tubulin first demonstrated that microtubules exhibit an unusual property called 'dynamic instability', whereby microtubules undergo prolonged periods of polymerization and depolymerization with transitions between the two states called catastrophe (from polymerization to depolymerization) and rescue (from depolymerization to polymerization)(Desai and Mitchison, 1997). *In vitro,* plus and minus ends both undergo dynamic instability over the same range of tubulin concentrations but display small quantitative differences.

As a result of interactions with specific binding proteins, the dynamic behavior of microtubules *in vivo* can differ dramatically from that described *in vitro*. A long list of proteins has been identified that bind at microtubule plus ends and regulate their dynamics. For example, MAP215 accelerates tubulin subunit addition at the plus end, EB1 promotes plus end growth and dynamicity, and Clip170 increases rescue frequency (Akhmanova and Steinmetz, 2008). Opposing these growth-promoting proteins are the

depolymerizing Kinesin-13 motors, which use ATP hydrolysis to induce a conformational change at plus ends to promote catastrophe (Moores and Milligan, 2006). The antagonistic actions of different +TIP proteins account for the more pronounced dynamic instability of microtubules *in vivo* compared to microtubules composed of pure tubulin *in vitro* (Kinoshita et al., 2001).

In contrast to the wealth of information on the microtubule plus end, the regulation of the microtubule minus end *in vivo* is poorly understood. In many cell types, the minus ends are clustered and anchored at a central microtubule-organizing center (MTOC). This organization has hindered visualization of their dynamics, in contrast with plus ends which are more easily viewed at the cell periphery by microscopy. Even in organisms and cell types that lack a central MTOC (e.g. S. pombe, D. melanogaster, A. thailinia, neurons, epithelial cells, and myotubes), the microtubule minus ends appear to be embedded in poorly characterized anchoring sites around the cell (Bartolini and Gundersen, 2006, Rusan and Rogers, 2009).

Occasionally, in animal cells, microtubules are released from an MTOC or break due to actomyosin forces, thereby allowing minus ends to be observed free from any nucleating material (Rodionov and Borisy, 1997, Vorobjev et al., 1999)(Yvon and Wadsworth, 1997)(Waterman-Storer and Salmon, 1997, Keating et al., 1997). The conclusion from these studies is that the vast majority (80-90%) of free microtubule minus ends are stable, neither visibly growing nor shrinking. A similar stability of minus ends has been observed in cytoplasmic extracts (Rodionov et al., 1999, Vorobjev et al.,

1997). Some minus ends, however, transition to rapid depolymerization resulting in the disappearance of the microtubule, and a very small percentage of microtubules treadmill through the cytoplasm (caused by simultaneous minus end shrinkage and plus end growth)(Rodionov and Borisy, 1997). Microtubule elongation from minus ends has not been reported *in vivo*. Thus, in contrast to the pronounced dynamic instability of plus ends, minus ends are mostly static and are indeed less dynamic than minus ends composed of pure tubulin *in vitro*. These results suggest that microtubule minus ends might be capped by some unknown protein(s) that suppresses subunit dynamics.

When I started in the Vale lab, Gohta Goshima and Nico Stuurman had completed a whole-genome RNAi screen for spindle morphology defects in Drosophila S2 cells. From this screen, they identified nine novel proteins that resulted in short spindles upon depletion. I performed follow-up studies on these genes, and discovered that depletion of the short spindle phenotype 4 protein, ssp4, in interphase resulted in a significant number of moving microtubule fragments that appeared throughout the cytoplasm (Goshima et al., 2007). I spent the next several years determining the mechanism of this protein. In the work that went into my thesis, I demonstrate that that Drosophila ssp4, which we renamed Patronin for the Latin 'patronus' (protector), protects microtubule minus ends *in vivo* against depolymerization by Kinesin-13. In the absence of Patronin, I found that microtubules release from their nucleation sites and treadmill throughout the cytoplasm, a result of unhindered minus end depolymerization. Furthermore, I demonstrated that purified Patronin selectively binds to and protects minus ends against Kinesin-13-induced depolymerization *in vitro*, demonstrating that Patronin alone is sufficient to confer minus

end stability. Thus, Patronin is the first protein demonstrated to cap and stabilize the microtubule minus end *in vivo*.

While I was working on Patronin, two papers on human homologs of Patronin were published. One demonstrated through computational homology searches that humans had three Patronin human homologs (Baines et al., 2009). The other, a very nice study by Meng *et. al*. demonstrated that one of these human homologs localized at microtubule minus ends in zonula adherens in epithelial cells (Meng et al., 2008), strongly suggesting that Patronin function is conserved.

In this thesis, Chapter 1 contains the work I did on characterizing Patronin's function. These experiments definitively demonstrate that Patronin is a microtubule minus end protector *in vivo* and *in vitro*. Chapter 2 contains experiments exploring Patronin's role *in vivo* and focuses on identifying interacting partners, particularly those involved in microtubule nucleation. In the conclusion I speculate on future directions and possible roles of Patronin in forming non-centrosomal microtubule arrays.

Chapter 1

Patronin selectively binds to and protects the microtubule minus end

Introduction

Microtubules are important for maintaining cell structure, providing platforms for intracellular transport, forming the spindle during mitosis, as well as other cellular processes. Microtubules are able to be involved in such a variety of functions because they are highly dynamic polymers. The microtubule filament is made up of α- and β-tubulin heterodimers. These heterodimers associate in a head-to-tail fashion to form protofilaments, and these protofilaments associate laterally to make a microtubule (Nogales and Wang, 2006). Microtubule undergo a process called dynamic instability, whereby the microtubule can polymerize, depolymerize and switch rapidly between the two phases in processes called catastrophe (switching from polymerization to depolymerization) and rescue (switching from depolymerization to polymerization)(Mitchison and Kirschner, 1984).

Both ends of the microtubules exhibit dynamic instability *in vitro* with roughly the same parameters under the same conditions (Desai and Mitchison, 1997). However, *in vivo*, minus ends often appear stable while plus ends remain dynamic (Dammermann et al., 2003). Interestingly, a long list of proteins has been identified that bind to and regulate different aspects of plus end dynamics (Lansbergen and Akhmanova, 2006). Meanwhile the minus end remains much more of a mystery. In order to form highly

complex and functional microtubule arrays, there must be some unknown protein(s) that regulate minus end stability. This is particularly important for cells that do not have central microtubule organizing centers, such as neurons and epithelial cells.

Drosophila S2 cells create non-centrosomal microtubule arrays in interphase, although they form centrosomes in mitosis (Rusan and Rogers, 2009). S2 cells are highly amenable to RNAi and microscopy, making them an ideal model organism in which to study microtubule minus end stability. In this Chapter, I detail experiments demonstrating that Patronin is the major microtubule minus end stabilizer in S2 cells. Patronin binds to and protects the minus end from the depolymerizing kinesin, Kinesin-13, *in vivo*. I also reconstitute Patronin's protective function *in vitro*, demonstrating that Patronin alone binds to minus ends and is sufficient to protect them from depolymerization by Kinesin-13s. Careful observation of microtubules in the absence of Patronin further demonstrate that minus end dynamics are regulated by competing actions of destabilizing and stabilizing proteins, as has been shown previously for the plus end. These studies further our understanding of how microtubule arrays are formed and regulated to achieve highly complex structures and functions.

Results

Depletion of Patronin results in free microtubules that move through the cytoplasm

Drosophila S2 cells do not have a central MTOC in interphase, but rather generate microtubules from multiple small nucleating sites, with microtubule plus ends generally visible at the cell periphery, while minus ends lies more centrally (Rogers et al., 2008; Rusan and Rogers, 2009). In wildtype cells, 'free' microtubules (where both the plus and minus end of the same microtubule are both clearly observed) are rarely found in the periphery (Figure 1A). In striking contrast, when Patronin was depleted by RNAi (Figure 2A), the interphase microtubule cytoskeleton became less dense (Figure 1A)(45% polymer decrease; Figure 2B) and the majority of cells had >5 free microtubules visible at the cell periphery (Figure 1A). Previously, we speculated that free microtubules might arise from increased severing after RNAi of Patronin (Goshima et al., 2007). However, we did not observe microtubule severing events in Patronin RNAi cells, and RNAi knockdown of microtubule severing proteins did not suppress the number of free microtubules seen after Patronin RNAi (Figure 2F).

Time-lapse observation of GFP-tubulin cells provided new insight into how Patronin affects microtubules. Free microtubules appeared to move in a linear manner within the cytoplasm (Figure 1B). In many cases, we observed microtubules releasing from sites of nucleation and moving towards the cell periphery, which might explain the appearance of free microtubules near the cell boundary (Figure 1A, 1C, 2C). Since

microtubules are nucleated at their minus ends, these observations indicated the free microtubules were 'moving' with their plus ends leading and their minus ends trailing. This conclusion is further supported by observations of EB1-GFP, which always localized to the leading end of the translocating microtubule in Patronin RNAi cells (Figure 1D).

Free microtubules move by treadmilling in Patronin-depleted cells

The movement of microtubules in the cytoplasm in Patronin depleted cells could result from either: 1) transport by an anchored minus end-directed motor protein (e.g. cytoplasmic dynein), or 2) microtubule treadmilling caused by tubulin addition at the plus end at a similar rate as tubulin loss at the minus end. To distinguish between these two mechanisms, we photobleached a section of a free GFP-labeled microtubule and observed how the bleach mark moved relative to the two microtubule ends. If the free microtubule is actively transported, the bleach mark should remain stationary relative to the plus and minus ends of the moving microtubule. Conversely, if the microtubule is treadmilling, the bleach mark should appear to move away from the plus end and get closer to the minus end. In Patronin-depleted cells, we observed the latter result; all plus ends moved away from the bleach mark (3.3 ± 0.3 μm/min; n = 20)(mean ± S.D.) while the minus ends moved closer (3.2 ± 0.3 μm/min; n = 20) and eventually passed through the bleached area (Figure 3A). These results indicate that microtubules move through the cytoplasm by treadmilling.

We next wanted to determine whether microtubule treadmilling occurs for any free microtubule or if this phenomenon requires the depletion of Patronin. In wildtype cells, it was possible to find an occasional free microtubule, but these did not translocate in the cytoplasm. When we photobleached a free microtubule from a wildtype cell, the bleach mark remained at a constant distance from the minus end (0.01 ± 0.07 μm/min; n = 10), while the plus end continued to polymerize (3.25 ± 0.24 μm/min; n = 10)(Figure 3A). This finding suggests that free microtubule minus ends are stable in wildtype cells, as has been observed in other cell types (Dammermann et al., 2003) and that the minus end depolymerization that gives rise to microtubule treadmilling requires the depletion of Patronin. We also examined whether minus end depolymerization occurred after RNAi depletion of g-tubulin, g-TuRC and g-TuSC components, since the g-TuRC complex has been shown to bind to microtubule minus ends *in vitro* (Moritz et al., 1995; Zheng et al., 1995; Wiese and Zheng, 2000). However, in these RNAi cells, free microtubules were rare and did not undergo treadmilling (Figure 2D).

To learn more about microtubule behavior after Patronin depletion, we measured the plus and minus end dynamics in wildtype and Patronin depleted cells. For the microtubule plus end, the rates of growth and shrinkage and the frequencies of catastrophe and rescue were similar under Patronin-depletion and wildtype conditions (Table 1). Thus, Patronin appears to have negligible effects on plus end dynamics. In contrast, minus ends displayed very different dynamics after Patronin depletion. In Patronin RNAi cells, minus ends of treadmilling microtubules often depolymerized at a rate of 3.9 ± 0.9 μm/min (mean ± S.D.), which is similar to the plus end polymerization

rate of 4.2 ± 1.3 μm/min (Table 1). The similarity in the rates of tubulin addition at the plus end and dissociation from the minus end explains why the lengths of treadmilling microtubules often remain relatively constant, with occasional shortening or lengthening when either the plus end or minus end pauses. We also observed a more rapid minus end depolymerization rate of 10.2 ± 2.2 μm/min, and occasionally individual microtubules would transition between the slow and fast depolymerization rates (Figure 2E). Interestingly, minus end depolymerization often halted when it reached the EB1-enriched microtubule plus end tip (Figure 4A, 20 of 30 depolymerizing microtubules paused for an average of 35.8 ± 13.1 sec), indicating that +TIP proteins might help the microtubule resist continued minus end depolymerization. After such a pause, the microtubule would either continue to depolymerize and disappear (11 of 20 microtubules) or resume plus end growth and increase in length (Figure 4A; 9 of 20 microtubules). In summary, microtubule minus ends can depolymerize at two rates *in vivo*: one similar to plus end growth (resulting in treadmilling) and a second more rapid rate that can lead to complete microtubule disappearance and may account for the sparser microtubule network after Patronin RNAi.

Depletion of the Kinesin-13 microtubule depolymerase, Klp10a, suppresses the Patronin phenotype in interphase and mitosis

The above results reveal that Patronin protects the microtubule minus end against depolymerization *in vivo*. We next wanted to determine if the depolymerization was an intrinsic property of the minus end or whether another protein was actively involved.

Kinesin-13s are microtubule depolymerizers that localize to both plus and minus ends *in vitro*, and *in vivo* bind to microtubule plus ends during interphase and promote their depolymerization (Desai et al., 1999; Hunter et al., 2003; Mennella et al., 2005). Kinesin-13s also promote the poleward flux of tubulin subunits towards the spindle pole during mitosis, a process that involves minus end tubulin turnover (Kwok and Kapoor, 2007, Rogers et al., 2004). To determine whether a Drosophila Kinesin-13 family member is involved in depolymerizing the microtubule minus ends after Patronin depletion, we performed double RNAi of Patronin with the three Drosophila Kinesin-13 genes (Klp10a, Klp59C, Klp59D) and examined the effect on interphase microtubule dynamics. Strikingly, co-depletion of Klp10a rescued the Patronin RNAi phenotype; the microtubule array was denser and free microtubules were no longer observed in the majority of the cells (Figure 3B, 2C). In contrast, double RNAi of either Klp59C or Klp59D with Patronin did not affect the number of free, treadmilling microtubules (Figure 3C). When a rare, free microtubule was found in a Patronin and Klp10a co-depleted cell, the minus end either remained stationary or appeared to grow, resulting in an increase in microtubule length. Interestingly, EB1-GFP localized to both ends of these growing microtubules, although it appeared more abundant at the presumed plus end at the cell periphery (Figure 4B). We also occasionally observed a transient localization of EB1-GFP at free microtubule minus ends in cells depleted of Patronin alone, which was accompanied by a pause in minus end depolymerizing and increase in microtubule length (Figure 4B). This, to our knowledge, is the first observation of *in vivo* minus end polymerization.

We also examined the interphase localization of Klp10a-GFP in Patronin-depleted cells. Previous studies showed that Klp10a-GFP localizes to microtubule plus ends prior to their catastrophe/depolymerization; the loading of Klp10a to growing plus ends is mediated by an interaction with EB1 (Mennella et al., 2005). In Patronin-depleted cells, we observed a prominent puncta of Klp10a-GFP tracking along the depolymerizing minus ends of treadmilling microtubules (Figure 3D). In cells co-expressing Klp10a-GFP and EB1-mCherry, we confirmed that more Klp10a is found at the depolymerizing end while EB1 is at the growing plus end (Figure 3E). This localization data supports the conclusion of the Klp10a rescue experiments indicating that Klp10a is actively depolymerizing minus ends in the absence of Patronin, and suggests this minus end localization is not dependent on EB1.

We next examined whether Klp10a is involved in producing the short spindle phenotype observed after Patronin depletion (Goshima et al., 2007). Wildtype spindles have a pole-to-pole length of 10.1 ± 1.7 μm (mean ± SD), which was reduced to 6.1 ± 1.3 μm after Patronin depletion (Figure 5A, 3B). A similar reduction was observed in acentrosomal mitotic spindle produced by centrosomin (Cnn) RNAi (Li and Kaufman, 1996)(9.6 ± 1.9 μm in Cnn RNAi cells and 6.7 ± 1.3 μm after Cnn/Patronin double RNAi (n = 35)), suggesting Patronin's function is not limited to the centrosome. Interestingly, we observed two distinct classes of short, bipolar spindles after Patronin RNAi: one in which the spindle had normal morphology with a clearly aligned metaphase plate, and another where the spindle appeared "collapsed" and the bipolar array penetrated across the metaphase plate (Figure 6B). Co-depletion of Klp10a and Patronin restored normal

morphology (Figure 5A, B) and produced longer spindles (12.4 ± 2.6 μm) than wildtype cells, a length comparable to Klp10a depletion alone (11.2 ± 2.2 μm). Conversely, co-depletion of Klp59C or Klp59D and Patronin, produced shorter spindles than wildtype cells (Figure 6A). These results suggest that Patronin protects microtubule minus ends against Klp10a-induced depolymerization during mitosis and that the balance of counteracting stabilizing and destabilizing forces at the minus ends governs spindle length (see Discussion).

Poleward flux of tubulin subunits during metaphase has been associated with minus end depolymerization by Klp10a and linked to the regulation of spindle length; less poleward flux results in longer spindle and vice versa (Rath et al., 2009). Depletion of Patronin resulted in an increased flux (2.03 ± 0.06 μm/min) over wildtype (1.44 ± 0.28 μm/min), thus explaining the shorter spindle. As previously reported, Klp10a RNAi caused a dramatic reduction in flux (0.68 ± 0.09 μm/min)(Laycock et al., 2006; Rath et al., 2009). Co-depletion of Patronin and Klp10a produced a flux (0.66 ± 0.03 μm/min) similar to Klp10a alone (Figure 5C), thus explaining the long spindle phenotype.

Taken together, our results suggest that Klp10a is actively depolymerizing free microtubule minus ends in interphase and mitosis and that the presence of Patronin is able to suppress this depolymerization activity.

GFP-Patronin localizes to microtubule nucleation centers

To learn more about Patronin's functions, we determined its intracellular localization. A polyclonal antibody made against the C-terminal region of Patronin, while having considerable background staining, showed that endogenous protein localizes to centrosomes in prophase, the midbody during cytokinesis, throughout the metaphase spindle, and to puncta in interphase that often overlap with microtubules (Figure 8C).

A GFP-Patronin fusion protein, which rescued the Patronin phenotype and thus is functional (Figure 8A), localized in punctae along microtubules in interphase, bundling them at moderate to high expression levels, and localized throughout the mitotic spindle (Figure 7A, Figure 8B). We also examined the localization of Patronin's three major domains: an N-terminal calponin homology domain (CH), a middle domain containing 3 predicted coiled-coils (CC), and a C-terminal microtubule binding domain (CKK domain (Baines et al., 2009)). The CH domain appeared diffuse throughout the cytoplasm (Figure 11A), while the CKK domain localized along all microtubules as previously reported (Baines et al., 2009)(Figure 7A). Interestingly, the central CC domain localized to small microtubule nucleating foci (Figure 7A) and occasionally along short stretches of microtubules.

We also visualized GFP-Patronin during the depolymerization and reformation of the microtubule cytoskeleton using the microtubule depolymerizing drug colcemid. After complete microtubule depolymerization, small foci containing both GFP-Patronin and

mCherry-tubulin were observed throughout the cytoplasm (data not shown). Sas-4 and γ-tubulin, established markers of microtubule nucleating centers, localized to similar foci in GFP-tubulin cells under the same conditions (data not shown). In the initial phase of microtubule regrowth, microtubules elongated out from these foci, eventually reforming the interphase microtubule array (Figure 7B). Therefore Patronin localizes to sites of new microtubule formation.

Purified Patronin specifically binds to and protects microtubule minus ends against depolymerization *in vitro*

Our *in vivo* studies revealed that Patronin stabilizes microtubule minus ends and protects them against Kinesin-13 depolymerization. To determine if Patronin alone is sufficient for such protection, we expressed and purified full-length GFP-Patronin-6xHis (224 kDa) from baculovirus infected Sf9 cells (Figure 9A) to test its activity *in vitro*.

We first wanted to establish how Patronin interacted with microtubules made from purified tubulin. We attached GFP-Patronin to a coverslip using a surface adsorbed anti-GFP antibody and then added GMP-CPP stabilized, rhodamine-labeled microtubules. Strikingly, the microtubules attached to the coverslip by only one end, resulting in filaments that swiveled in space while anchored at a single point (Figure 9B). In most cases, a clear spot of GFP-Patronin co-localized with the anchored end of the microtubule (asterisks, Figure 9B). Microtubules did not bind to the coverslip surface in the absence of Patronin and attached along their length when bound by anti-tubulin

antibody or kinesin (data not shown). To determine if Patronin preferentially bound to the microtubule plus or minus end, microtubule gliding was induced by introducing kinesin or dynein to the assay. With kinesin, the Patronin-bound end became the leading end as kinesin moved the microtubule across the glass (128 out of 130 pre-anchored microtubules exhibited this polarity)(Figure 9C). The leading end of gliding microtubules also frequently stopped, presumably due to rebinding to Patronin, causing the microtubule to buckle due to the pushing force of kinesin (asterisk in Figure 9C). Conversely, when dynein was added, the Patronin-bound end now became the trailing end of the gliding microtubule (138 out of 139 microtubules)(Figure 9C). These results show that Patronin binds highly selectively to the microtubule minus end *in vitro*.

To further confirm these conclusions, we sought to visualize GFP-Patronin bound to the microtubule. In this assay, we first attached kinesin or dynein to the coverslip and then added GMP-CPP rhodamine-labeled microtubules along with purified GFP-Patronin. By TIRF microscopy, GFP-Patronin most often bound at only one end of the microtubule. With kinesin pushing the microtubule, GFP-Patronin was on the leading microtubule end (of 84 microtubules with bound GFP-Patronin, 80 had a GFP-Patronin spot at the minus end, 1 was at the plus end, and 3 appeared internal)(Figure 9D). With dynein transporting the microtubule, GFP-Patronin was at the trailing end (of 101 microtubules with bound GFP-Patronin, 91 were at the minus end, 4 were at the plus end, and 6 appeared internal)(Figure 9E). Thus, by direct observation, GFP-Patronin binds selectively to the minus end.

We next tested whether purified Patronin is sufficient to protect minus ends against Kinesin-13 induced depolymerization using a reconstituted assay with purified MCAK motor domain from P. falciparum (P.f. MCAK) (homologue of Klp10a, Moores et al., 2002)(Figure 10A, 6B). GMP-CPP polarity marked microtubules were adhered to the coverslip via anti-rhodamine antibody, and P.f. MCAK was added in the presence or absence of Patronin. Without Patronin, both ends of the microtubule depolymerized (plus end: 2.5 ± 0.4 μm/min, minus end: 1.8 ± 0.7 μm/min; comparable to rates reported previously *in vitro* (Hunter et al., 2003; Desai et al., 1999; Cooper et al., 2009). In the presence of purified Patronin, however, depolymerization from the plus end still occurred (2.2 ± 0.3 μm/min) while depolymerization from the minus end was negligible (0.01 ± 0.06 μm/min)(Figure 10A, 6B). We also observed selective minus end stabilization with Patronin and full-length hamster MCAK (C.g. MCAK)(Figure 10C). Higher concentrations of P.f. or C.g. MCAK, lead to the depolymerization of a portion of minus ends, suggesting that there is a competition between Patronin and MCAK for minus end binding (Figure 10C). The full-length MCAK competed more effectively than the motor domain, likely because of its higher association rate ((Cooper et al., 2009). We also performed an alternative assay in which the microtubule minus end was anchored to surface adhered Patronin and a solution of P.f. MCAK was added. Once again, MCAK depolymerized the plus end rapidly, whereas the Patronin-anchored minus end did not shorten at our level of detection (Figure 11A, 11B, 11C). In summary, our *in vitro* studies reveal that purified Patronin binds selectively to the microtubule minus end and this binding confers protection against Kinesin-13-induced microtubule depolymerization.

Discussion

Microtubule minus end dynamics has remained one of the least well understood properties of the microtubule cytoskeleton. Here, through *in vivo* and *in vitro* approaches, we have demonstrated that Patronin binds with high selectivity to microtubule minus ends and acts as a "cap", stabilizing these ends and protecting them against the actions of microtubule depolymerases. The consequence of losing Patronin-mediated capping in S2 cells is dramatic. During interphase, the microtubule density decreases and microtubules released from nucleating sites treadmill through the cytoplasm. During mitosis, the spindle becomes significantly shorter and in some cases collapses to a shape that more resembles a monopolar spindle. In addition to clarifying the role of Patronin, our studies also provide new insight into the regulation of microtubule minus end dynamics. We demonstrate that minus ends are substrates for capping (Patronin), destabilizing (Kinesin-13), and possibly growth promoting or stabilizing (EB1) activities, as has been demonstrated for the microtubule plus end. The behavior of minus ends reflects a net balance of these actions, which plays an important role in the overall organization of the microtubule cytoskeleton.

Patronin mechanism

Patronin binds with high selectivity to the minus end of microtubules (>92% from our *in vitro* experiments), suggesting that it recognizes some unique, exposed feature at this end. In the polar microtubule, α-tubulin faces the minus end while β-tubulin faces

the plus end (Mitchison, 1993). Thus we speculate that Patronin recognizes features of α-tubulin that are normally buried at the α/β interface but are exposed at the end of the microtubule. Consistent with this possibility, an anti-a-tubulin antibody has been produced that binds selectively to the microtubule minus end (Fan et al., 1996). Interestingly, selective minus end binding appears to require the cooperation of multiple regions of the Patronin protein, since the C-terminal CKK domain alone binds uniformly along the microtubule surface (Figure 7A)(Baines et al., 2009).

An important functional consequence of Patronin binding to minus ends is protection against Kinesin-13 depolymerization. Kinesin-13 destabilizes microtubule ends by bending microtubule protofilaments, causing them to lose lateral interactions (Moores and Milligan, 2006). Patronin might sterically block Kinesin-13 binding and/or strengthen the lateral interactions of protofilaments, rendering minus ends resistant to depolymerization. A better understanding of how Patronin caps and protects minus ends will require higher resolution structural information of the Patronin-microtubule minus end complex.

Regulation of microtubule minus end dynamics *in vivo*

A large and still growing list of proteins have been discovered that associate with microtubule plus ends and many exhibit opposing effects on microtubule dynamics (Akhmanova and Steinmetz, 2008; Howard and Hyman, 2007), which gives rise to the high dynamicity of plus ends *in vivo* and enables cells to rapidly restructure their

microtubule cytoskeleton. The dynamics of microtubule minus ends *in vivo* has not been as well studied as plus ends, particularly at the level of single microtubules. In the few studies where minus ends have been observed in animal cells, they have been reported to be mostly stable (neither growing or shrinking; (Rodionov and Borisy, 1997; Yvon and Wadsworth, 1997; Waterman-Storer and Salmon, 1997b). Minus end shrinkage and microtubule treadmilling, however, is common in Arabidopsis (Shaw et al., 2003; Ehrhardt, 2008). In contrast, microtubule minus ends composed of pure tubulin grow, shorten, and exhibit dynamic instability (Desai and Mitchison, 1997). The discrepancy between such *in vitro* dynamicity and *in vivo* stability suggests the presence of a minus end capping factor. γ-TuRC interacts directly with the microtubule minus end (Moritz et al., 1995; Zheng et al., 1995; Wiese and Zheng, 2000). However, while γ-TuRC has a clear role in microtubule nucleation *in vivo*, it is uncertain whether it remains bound to and stabilizes minus ends after the microtubule is nucleated. Indeed, we feel that this may not be the case, at least in Drosophila, since γ-TuRC RNAi knockdown does not greatly alter the appearance of the interphase array (Bouissou et al., 2009), produces elongated rather than short mitotic spindles (Vérollet et al., 2006), and does not generate free, treadmilling microtubules (Figure 2D, 6A). Another protein, ninein, plays a role in anchoring microtubules to MTOCs and other sites within cells (Delgehyr et al., 2005); however this interaction appears to be facilitated by γ-TuRC and ninein has not been shown yet to interact directly with minus ends. RNAi of other genes that produced a short spindle phenotype (Goshima et al., 2007) or centrosomal proteins (Sas-4, SAK, Asp, and Cnn, data not shown) did not give rise to a microtubule treadmilling phenotype indicative

of minus end instability. Thus, Patronin is the only protein for which minus end capping activity as been demonstrated *in vivo*.

Our experiments also demonstrate that in the absence of Patronin-mediated capping, microtubule minus ends *in vivo* exhibit the range of behaviors seen *in vitro* (polymerization, depolymerization, catastrophe, and rescue) and also are acted upon by previously identified plus end binding proteins. EB1 has been used as canonical marker of microtubule plus ends *in vivo*. Here, we show that EB1-GFP can interact with microtubule minus ends during episodes of subunit addition (Figure 4B). Kinesin-13, which binds to plus ends and induces their catastrophe, has been suggested to depolymerize microtubule minus ends during mitosis based upon its role in spindle flux (Rogers et al., 2004), but has not been directly visualized at microtubule minus ends. Here, we show that in the absence of Patronin, the Kinesin-13 Klp10a-GFP binds to and tracks along depolymerizing minus ends and is also required for this depolymerization (Figure 3). In Patronin-depleted cells, the actions of Klp10a appear to dominate over any minus end growth promoting factors, as most microtubule minus ends undergo depolymerization and only rarely display brief periods of growth. In summary, microtubule minus ends can grow, depolymerize or be capped *in vivo* and the balance of proteins that promote these activities govern the behavior of microtubule minus ends in cells.

The importance of balancing stabilizing and destabilizing activities on microtubule ends is illustrated in the mitotic spindle. Net polymerization occurs at

microtubule plus ends near the kinetochore and net depolymerization occurs at minus ends at the poles, which results in a poleward flux of tubulin subunits within the microtubule lattice (Kwok and Kapoor, 2007; Rogers et al., 2004). The overall balance of polymerizing and depolymerizing activities of microtubule-associated proteins governs the size and shape of the spindle (Goshima et al., 2005; Dumont and Mitchison, 2009). Studies in several organisms have implicated Kinesin-13s as major regulators of mitotic microtubule length, spindle size, and poleward flux (Mitchison et al., 2005, Rath et al., 2009, Kwok and Kapoor, 2007). Our results suggest that Patronin provides a "brake" rather than a full block on the minus end depolymerizing actions of Kinesin-13. In the absence of Patronin, Kinesin-13 is unchecked, resulting in a higher flux rate and shorter, sometimes collapsed spindles. With the depletion of both Patronin and Kinesin-13, flux is low and spindle length is longer than normal. These results imply that microtubule minus ends are not completely protected by Patronin but are subject to competing activities of Patronin and Kinesin-13, as we also demonstrate *in vitro* (Figure 10C). Thus, a balance of Patronin and Kinesin-13 actions on microtubules minus ends governs the length of the mitotic spindle.

The Patronin family and minus end capping in acentrosomal microtubule arrays

A single Patronin gene is found in invertebrate genomes and clear homologues do not exist or are difficult to identify in non-metazoan organisms. After Patronin (then named ssp4) was first described in Drosophila (Goshima et al., 2007), three vertebrate homologues with the same domain organization and sequence identity were reported and

have been called the CAMSAP/ssp4 family of proteins (the three vertebrate branches are referred to as CAMSAP1, CAMSAP2, and CAMSAP3; (Baines et al., 2009)). All Patronin-related genes have a characteristic domain organization of an N-terminal calponin homology (CH) domain, a long central domain with interspersed predicted coiled-coil regions, and a C-terminal microtubule-binding domain (termed the CKK domain), which is the most highly conserved region of the polypeptide (Baines et al., 2009). While this work was in progress, vertebrate CAMSAP1 and a CAMSAP3 member, Nezha, were reported to interact with microtubules (Baines et al., 2009, Meng et al., 2008). Meng et. al. (2008) found that Nezha localizes specifically at microtubule minus ends located close to adherens junctions in epithelial cells and bound preferentially to the minus end *in vitro* (67% of microtubule-associated Nezha). However, their study did not explore whether Nezha affected the dynamics of microtubules or influenced the organization of the microtubule cytoskeleton. If the vertebrate homologues also are found to protect microtubule minus ends as shown here for Drosophila Patronin, we suggest that the currently named CAMSAP/ssp4 family be renamed as the Patronin family, retaining the phylogenetic classification of the three vertebrate branches (Patronin 1, 2, and 3)(Baines et al., 2009).

Minus end capping has been proposed to be particularly important for the formation and organization of non-radial, acentrosomal interphase microtubule arrays (Dammermann et al., 2003; Bartolini and Gundersen, 2006). The roles of the three Patronin family members in vertebrates are not yet defined, but they may have evolved to interact with distinct partners for localizing microtubule minus end capping/anchoring

activities to distinct subcellular regions in epithelial cells (Meng et al., 2008), neuronal cells (Berglund et al., 2008), and other cell types with acentrosomal arrays. Thus, the three Patronin family members might provide new molecular tools for probing the organization and function of microtubules in different vertebrate cells types.

Experimental Procedures

Cell culture, cell lines, plasmids, and RNAi

Drosophila S2 cells (UCSF) were cultured and incubated with dsRNA as previously described (Goshima and Vale, 2003). Unless noted, cells were treated with dsRNA for 4 days, and when indicated were treated additional dsRNA at day 4 and analyzed at day 8. Patronin was cloned from a S2 cell cDNA pool into the pENTR/D-TOPO vector (Invitrogen) and moved into vectors with metallothionein promoters (pMT) and N- or C-terminal GFP or mCherry vectors (N- and C-terminal fusions produced the same results). Patronin domain constructs were cloned in correspondence to the amino acids listed in Figure 4. Previously constructed pMT-EB1-GFP, pAC-mCh-tubulin, pMT-Klp10a-GFP, and an EGFP-α-tubulin cell lines were used (Mahoney et al., 2006)(Goshima and Vale, 2005)(Goshima et al., 2007)(Rogers et al., 2002). Stable cell lines were made using Effectene (QIAGEN) according to the manufacturers instructions. Expression from pMT vectors was induced by adding 50 μM $CuSO_4$ for 18-24 hr.

dsRNA sequences for RNAi

DsRNAs were made by first PCR from a cDNA S2 cell library with the following primers containing T7 promotors.

Patronin: (left)TAATACGACTCACTATAGGGCATCGACGCCTTCACAATAC

(right) TAATACGACTCACTATAGGGGCCCATACACGATTTCATTTCC

Klp10a (left)TAATACGACTCACTATAGGGATTGGGCAATGTGTTATTAGGC

(right)TAATACGACTCACTATAGGGGGGAGAAAGAGAAAGAGATCGG

Patronin3'UTR:(left)TAATACGACTCACTATAGGGCGATTCGGATGCAGAAGGG

TGGCGGC

(right) TAATACGACTCACTATAGGGCGACTTTGGCTGCGGCCCATACACG

Additional sequences can be found at http://rnai.ucsf.edu

RNA was generated using an Ambion T7 MEGASCRIPT kit, annealed, and diluted to ~1 μg/μl.

Antibody production and immunostaining

A region of the *patronin* gene corresponding to amino acids 1363-1687 was cloned into a pENTR/D-TOPO vector (Invitrogen) and moved into pDEST17 vector (Invitrogen), and protein expression was induced in BL21 DE3 cells (Invitrogen). The expressed proteins were purified on a Ni-NTA column (Qiagen) and used for injecting rabbits (Covance). Polyclonal anti-Patronin antibodies were purified on an Actvated Sepharose 4 Fast Flow CnBr column (Pharmacia Biotech) containing the immobilized antigen. To isolate protein from S2 cells after RNAi treatment, Laemmli sample buffer was added to cells and western blotting was performed as previously described (Rogers et al., 2003) probing at 4° C overnight with 1:1000 anti-Patronin polyclonal antibody and 1:1000 anti-actin monoclonal antibody (JLA20, Calbiochem).

For immunofluorescence, cells were fixed at -20° C with a 90% methanol, 3.2% paraformaldehyde, and 5 mM NaCitrate solution, blocked with 10% normal goat serum in PBST (0.1% Triton X-100 in PBS) and incubated with 1:1000 anti-Patronin, 1:1000 anti-α-tubulin (DM1α, Sigma, or YOL1, Serotec) and 1:1000 anti-γ-tubulin (GTU-88,

Sigma) at 4° C overnight. Cells were incubated with secondary antibodies (AlexaFluor-488, AlexaFluor-555, and AlexaFluor-647 Molecular Probes, all at a 1:1000 dilution) for 1 hr, washed in PBST and mounted under fluorescence mounting medium (Dako). Cells were imaged on the Zeiss and Nikon microscopes described above using μManager software. Spindle lengths were measured using ImageJ software (NIH) to measure pole-to-pole distance.

Live cell imaging

Cells were plated on Con A (Sigma) coated MatTek dishes for 1 hr unless noted. Live cell imaging was performed by spinning disk confocal microscopy or occasionally by TIRF microscopy (noted in the legends). Microscope equipment is described in the Suppl. Methods. For the photobleaching experiments, GFP-tubulin cells were imaged on an LSM 510 or 710 (Carl Zeiss, Inc.)(63x 1.4 NA objective). Two or three imaging scans were performed with a 488 nm laser at 1.1% power before a selected area was bleached. On the LSM 510, bleaching was achieved with a 488 nm Argon laser at 100% laser power for 4 iterations, while on the LSM710 a 405 nm laser at 45% power was used for 2 iterations. After the photobleach, scans were taken at 488 nm (1.1% power) every 3 sec. The position of a bleach mark relative to microtubule ends or within a spindle (flux measurements) was measured over time using ImageJ.

Microscopy

Spinning disk microscopy was performed with a Zeiss Axiovert 200M equipped with a 100x 1.45 NA oil objective and a cooled charged-coupled device camera (Orca II ERG,

Hamamatsu Photonics) or an EM charged-coupled device camera (C9100-13; Hamamatsu Photonics). The 488-nm line of an argon laser or 561-nm line of a krypton laser was used for illumination, attached to a spinning-disk confocal scan head (CSU10; Yokogawa; obtained from Solamere, Inc.). TIRF microscopy was performed on an inverted microscope (TE2000U, Nikon) equipped for TIRF with a 100x 1.49 NA objective, a back-thinned electron multiplying CCD camera (iXon^{EM}+, Andor), using 491-nm diode and 561-nm diode lasers. Cells were flattened onto the coverslip with a 170 μm-thick 2% agarose layer (Kner et al., 2009). For all time-lapse *in vivo* experiments, images were acquired every 3 s using μManager software unless noted (www.micro-manager.org)(Stuurman et al., 2007). For images showing two colors, brightness was adjusted in each channel separately before merging (see figure legends).

In vitro microtubules

GMP-CPP stabilized microtubules were made by mixing unlabeled bovine brain tubulin with rhodamine-labeled tubulin (Cytoskeleton) at a 14:1 ratio with 1.5 mM GMP-CPP and 1 mM DTT in BRB80 (80 mM PIPES (pH 6.8), 1 mM $MgCl_2$, 1 mM EGTA), and incubated at 37° C for 2 hr.

GMP-CPP polarity marked microtubules were made by first making GMP-CPP stabilized 'seeds' by mixing 2:1 ratio of unlabeled:rhodamine-labeled tubulin with 1.5 mM GMP-CPP and 1 mM DTT in BRB80, and incubating the mixture at 37° C for 1 hr. After this incubation, 1.5 μl of the seeds were added to a 25 μl solution containing 2.5 μl of a 20:1

unlabeled:rhodamine-labeled tubulin mixture with 1.5 mM GMP-CPP and 1 mM DTT in BRB80, and incubated at 37ºC for 2 hr.

***In vitro* assays**

GFP-Patronin with a C-terminus 6xHIS tag was expressed using the BaculoDirect system (Invitrogen). Sf9 cells were infected with P3 virus for 3 days and harvested. GFP-Patronin-6xHis was purified on a NiNTA column (Qiagen); the eluted protein was dialyzed overnight into 50 mM Tris-HCl pH 8, 150 mM KAcetate, 1 mM DTT and 10% glycerol and stored in LN_2.

Flow cells were used for all *in vitro* assays. For the anchoring assay, anti-GFP antibody was adhered to the coverslip and 150 nM GFP-Patronin was added for 5 min. Coverslips were blocked with 1 mg/ml casein solution, after which a solution of GMP-CPP stabilized rhodamine-microtubules (See Supp. Methods), an oxygen scavenging mixture (catalase, glucose oxidase, and glucose), and 1 mg/ml casein in BRB80 was added (referred to as the 'microtubule solution'). To determine the polarity of the anchored microtubule, the experiment was repeated with the following changes: a mixture of anti-GFP and anti-GST antibody was adhered to the coverslip, and after microtubules were anchored by Patronin, K560 kinesin (Woehlke et al., 1997) or GST-D4.4 dynein (Reck-Peterson et al., 2006), an oxygen scavenger mix and 5 mM ATP was added.

For the motility assays, a coverslip with immobilized K560 kinesin or GST-D4.4 dynein (via anti-GST) was blocked with 1 mg/ml casein and the microtubule mixture plus 6 nM GFP-Patronin and 5 mM ATP was added.

For the Kinesin-13 depolymerization assay, polarity marked GMP-CPP rhodamine-microtubules (See Supp. Methods) were anchored to the coverslip with an anti-rhodamine antibody. The indicated concentration of Kinesin-13 (either the MCAK motor domain from P. falciparum (purified as described in (Moores et al., 2002)) or full length hamster MCAK obtained from Linda Wordeman (Cooper et al., 2009)) was added with 5 mM ATP in BRB80 with an oxygen scavenger mix. Images were taken at 20 s intervals on the TE2000U Nikon microscope using a 40x 1.3 NA objective and Nikon intensilight. Microtubule lengths were measured using ImageJ software.

Nucleation assays

A solution of 8 mg/ml, 4 mg/ml, or 3 mg/ml unlabeled tubulin along with 0.5 mg/ml Rhodamine-tubulin with 0.12 mM GTP in BRB80 with and without 50 nM Patronin was incubated at 37° C for 15 minutes, fixed with 45 µl 1% Glutaraldehyde in BRB80, and 10 µl of this solution was added to 90 µl 70% glycerol in BRB80. The solution was pipetted onto coverglass and the number of microtubules from 10 fields was scored.

MCAK depolymerization assay for Figure 11

We prepared segmented GMP-CPP stabilized microtubules for these assays in order to have an internal marker for measuring the microtubule depolymerization from each end. First, GMP-CPP stabilized 'seeds' were made mixing 3:1 ratio of unlabeled:rhodamine-labeled tubulin with 1.5 mM GMP-CPP and 1 mM DTT in BRB80, and incubating the mixture at 37° C for 45 min. After this incubation, 2 μl of the mixture was added to a 20 μl solution of 14:1 unlabeled:labeled tubulin with 1.5 mM GMP-CPP and 1 mM DTT in BRB80, and incubated at 37° C for 2 hr. In this assay, microtubules were anchored at one end to the coverslip by GFP-Patronin as shown in Fig. 5B. After addition of the GMP-CPP segmented microtubules, 4 μM of the MCAK motor domain from P. falciparum (purified as described in (Moores et al., 2002) was added with 5 mM ATP in BRB80 with an oxygen scavenger system. In the control assay, microtubules were anchored to the coverslip by an anti-tubulin antibody (YOL1, Serotec) before addition of Kinesin-13. For the plus and minus end depolymerization measurements, either K560 or GST-dynein was adhered to the coverslip (see Experimental Procedures), and subsequently the microtubule mixture was added, followed by addition of Kinesin-13. Images were taken at 20 sec intervals using a TE2000U Nikon microscope using a 40x 1.3 NA objective and Nikon intensilight. Microtubule lengths were measured at different time points using ImageJ software.

Figure Legends

Figure 1. Depletion of Patronin results in free microtubules that move through the cytoplasm

Time-lapse microscopy of wildtype and Patronin-depleted GFP-tubulin Drosophila S2 cells. (A) Patronin-depleted cells have numerous 'free' microtubules (both the plus and minus end of the same microtubule are clearly visible, arrows) which are rarely seen in wildtype cells and also have a sparser microtubule network (insert shows a region with several free microtubules). The right side shows the quantitation of free microtubules per cell from two independent experiments; colored bars indicate the percentage of cells with the number of indicated free microtubules observed (n = 200 cells per experiment; SEM <6%). Scale bars, 10 μm. (B) Time-lapse TIRF microscopy of Patronin-depleted GFP-tubulin cells demonstrates that free microtubules move throughout the cytoplasm (colored arrows follow the motion of the leading end of three microtubules). Scale bar, 10 μm. (C) In Patronin-depleted cells, microtubules (arrows) release and move away from the centrosome (prophase cell). Scale bar, 5 μm. (D) In cells co-expressing EB1-GFP (green) and mCherry-tubulin (red), EB1 localizes to the leading end of moving microtubules (arrows), indicating that this is the microtubule plus end. Brightness was adjusted in each color channel separately. Scale bar, 5 μm.

Figure 2. Characterization of free microtubule phenotype in Patronin depleted cells

(A) Western blot of 4- and 8-day Patronin depletion by RNAi. Total protein extracts of control or Patronin dsRNA treated cells were analyzed using an affinity purified, anti-

Patronin antibody and a monoclonal anti-actin antibody. (B) Quantitation of microtubule polymer content in wildtype and Patronin RNAi cells. GFP-tubulin cells were allowed to spread on Con A -coated coverglass, after which they were briefly (15 sec) fixed with 4% paraformaldehyde in BRB80, permeabilized with 0.5% Triton X-100 in BRB80 for 5 min, and fixed again for 20 min with 4% paraformaldehyde in BRB80. The mean pixel intensity for each cell was calculated using ImageJ and the background mean pixel intensity was subtracted to get the reported values. The mean and S.E.M are shown from two independent experiments (n > 100 cells per experimental condition). (C) In interphase Patronin-depleted cells, free microtubules originate by releasing and moving away from small nucleating foci (images taken using TIRF microscopy). (D) Quantitation of the percentage cells with greater than 5 free microtubules shows that depletion of g-tubulin and g-TuRC components does not result in free microtubules. The mean and S.E.M. is shown from two independent RNAi experiments (n = 100 cells scored per experiment). (E) The minus ends of individual, treadmilling microtubules in Patronin-depleted cells can occasionally make an abrupt transition between slow and fast depolymerization rates. Symbols in each panel track the linear positions of the plus (square) and minus (triangle) ends of a single, free microtubule as it treadmills in the cell over time. The lines indicate segments of continuous depolymerization over 3 or more time points. (F) Quantitation of the percentage cells with greater than 5 free microtubules shows that RNAi co-depletion of Patronin with severing proteins does not rescue the Patronin phenotype. The mean and S.E.M. is shown from two independent RNAi experiments (n = 100 cells scored per experimental condition).

Figure 3. Free microtubules move by Klp10a-mediated treadmilling in Patronin-depleted cells

(A) Photobleaching a mark in the middle of moving microtubules in Patronin RNAi cells reveal that the bleach mark is stationary and the trailing minus end moves towards the bleach mark (see arrows)(n=20). This indicates that the apparent motion of microtubules occurs through simultaneous tubulin polymerization at the plus end and depolymerization at the minus end. In wildtype cells, the bleach mark in a rare free microtubule remains stationary relative to the minus end, indicating that it is neither polymerizing nor depolymerizing (n=10). Scale bars, 10 μm. (B) Comparison of GFP-tubulin cells depleted of Patronin alone or both Patronin and Klp10a. Cells co-depleted of Patronin and Klp10a have a wildtype-like microtubule network and rarely have free microtubules. Scale bar, 10 μm. (C) Quantitation of the percentage of cells with >5 free microtubules shows that co-depletion of Patronin and Klp10a, but not Klp59C or Klp59D, rescues the Patronin RNAi phenotype. The mean and SEM is shown from two independent experiments (n=200 cells per experiment). (D) In Patronin-depleted cells co-expressing Klp10a-GFP (green) and mCherry-tubulin (red), Klp10a localizes to and tracks along the depolymerizing minus end of treadmilling microtubules (arrows). Scale bar, 5 μm. (E) In Patronin-depleted cells co-expressing Klp10a-GFP (green) and EB1-mCherry (red), Klp10a localizes to the trailing end, while EB1 localizes to the leading end of treadmilling free microtubules (frame from a time-lapse sequence). Scale bar, 5 μm. Brightness was adjusted in each color channel separately.

Figure 4. EB1 localizes to plus and minus ends of microtubules *in vivo*

Time-lapse microscopy of free microtubules in Patronin-depleted cells co-expressing EB1-GFP (green) and mCherry-tubulin (red) showed that (A) free microtubules depolymerizing from their minus end occasionally pause (21-42 s) when they reach the EB1-GFP enriched plus end tip, indicating this region resists minus end depolymerization (20 of 30 depolymerizing microtubules paused for an average of 35.8 ± 13.1 sec). In this case, after the pause, the minus end elongates (42-93 s)(9 of 20 scored microtubules exhibited this behavior). In other cases, the minus end depolymerization continues and the microtubule disappears (not shown)(11 of scored 20 microtubules exhibited this behavior). Arrows point to the microtubule plus and minus end. Brightness was adjusted in each color channel separately. (B) EB1-GFP can bind to the minus end in Patronin RNAi cells. In the cases where EB1-GFP is clearly observed at a minus end, the microtubule minus end appears to pause or increase in length (arrows point to EB1-GFP at the plus (top) and minus (bottom) ends). In Patronin and Klp10a co-depleted RNAi cells, EB1-GFP appears more frequently at the minus ends of free microtubules. After Klp10a depletion, growth at microtubule minus ends occurs for longer periods of time until a plus or minus end catastrophe occurs or the minus end moves into the cell body and is no longer visible. Arrows point to EB1-GFP at the plus (top) and minus (bottom) ends. Scale bars, 5 μm.

Figure 5. Depletion of Klp10a suppresses the Patronin phenotype in mitosis

(A) Co-depletion of Patronin and Klp10a rescues the short spindle phenotype observed in Patronin-depleted cells and results in elongated spindles similar to those seen in Klp10a-

depleted cells. Scale bar, 10 μm. (B) The mean pole-to-pole metaphase spindle length under each condition was quantified for two independent experiments (n>60 spindles per condition; error bar, SEM; p<0.001 for each reported condition). (C) The flux of tubulin towards the spindle poles was measured by photobleaching a ~1 mm stripe in the GFP-tubulin spindle and tracking its movement. The mean flux rates were quantified under each condition from two independent experiments (n=20 spindles per condition; error bar, SEM; p< 0.001 for each reported condition except the pair of Klp10a RNAi and Klp10a/Patronin RNAi flux (p<0.9)). Thus poleward flux is increased after Patronin depletion and decreased below wildtype levels when Patronin and Klp10a are co-depleted.

Figure 6. **Quantitation of spindle length and characterization of spindle morphology** (A) Measurements of spindle length demonstrate that co-depletion of Patronin with Klp10a, but not with Klp59C or Klp59D, rescues the short spindle phenotype. Depletion of g-TuRC components result in elongated spindles. The mean pole-to-pole metaphase spindle length under each condition is quantified from two independent experiments (n > 55 spindles per condition; error bar, S.E.M). (B) Loss of Patronin by RNAi results in a higher percentage of short bipolar mitotic spindles that do not have a clear metaphase plate ('collapsed'). Cells were immunostained for α-tubulin (red) and γ-tubulin (green). Representative examples of short and collapsed bipolar spindles are illustrated, and the scoring of spindle phenotypes from two independent experiments is shown on the left (n = 500 spindles per experimental condition, S.E.M. from the mean of the two experiments is <2%).

Figure 7. GFP-Patronin localization and domain analysis

(A) Co-expression GFP-fusions of full-length Patronin (TIRF microscopy) or Patronin domains with mCherry-tubulin (merge: GFP-Patronin in green and mCherry-tubulin in red). Localization patterns are discussed in the text. Scale bars, 10 μm. (B) Time-lapse microscopy of GFP-Patronin (green) and mCherry-tubulin (red) expressing cells re-growing their microtubule network after washout of the microtubule depolymerizing drug colcemid (time after washout is indicated). The inserts correspond to the box at 34 min. Patronin and tubulin localize to small foci, which serve as points of microtubule nucleation during the reformation of the cytoskeleton.

Figure 8. **Characterization of Patronin *in vivo*.** (A) mCherry-Patronin can rescue the Patronin RNAi phenotype when expressed in cells where the endogenous Patronin is depleted by dsRNA against the 3'UTR. The mCherry-Patronin expressing cell (top) has a normal microtubule network and lacks free, peripheral microtubules as opposed to the cell that also lacks Patronin and is not expressing mCherry-Patronin (bottom). The left side shows the quantitation of free microtubules per cell from three independent experiments; colored bars indicate the percentage of cells with the number of indicated free microtubules observed in their peripheral cytoplasm (n = 232 cells per condition, the S.E.M. from the mean of the three experiments is <5%) Scale bar, 10 μm. (B) GFP-Patronin (green) localizes diffusely throughout the mitotic spindle (mCherry-tubulin (red) image also is shown). Scale bar, 10 μm. (C) The localization of endogenous Patronin was determined by immunostaining Drosophila S2 cells for Patronin with an affinity-

purified rabbit polyclonal antibody (green) or α-tubulin (red) in interphase, prophase, metaphase, and cytokinesis.

Figure 9. Purified Patronin selectively binds to microtubule minus ends *in vitro*

(A) Purified GFP-Patronin-6xHis analyzed by SDS polyacrylamide gel electrophoresis and stained with Coomassie blue. Immunoblot analysis reveals that lower band of the doublet is Patronin lacking the GFP (not shown). (B) When GFP-Patronin is attached to a coverslip with anti-GFP antibody, it binds GMP-CPP stabilized rhodamine-labeled microtubules by one end. Asterisks indicate the site of microtubule anchoring, which often overlaps with a GFP-Patronin spot. Scale bar, 10 μm. (C) To reveal which microtubule end was anchored to GFP-Patronin, kinesin or dynein was added after microtubule anchoring. Arrows follow a microtubule that was initially anchored by one end and then bound along its length to the motor-covered surface. With kinesin, the formerly anchored end is leading moving end (until the leading end reattaches and the microtubule buckles (asterisk, 60 s); with dynein, the formerly anchored end is trailing. These assays reveal that microtubules are anchored to surface-bound Patronin selectively at their minus end (see statistics from three independent experiments in the text). Scale bar, 5 μm. Conventional kinesin (D) or dynein (E) microtubule gliding assays in the presence of GFP-Patronin (6 nM; green) demonstrate that GFP-Patronin binds selectively to the minus end. In the kinesin assay, GFP-Patronin (green) is most frequently observed at the leading end of gliding microtubules, while in the dynein assay, it resides at the trailing end. The results from three independent experiments indicate that GFP-Patronin binds selectively to the minus end. Scale bars, 10 μm.

Figure 10. GFP-Patronin protects microtubule minus ends from Kinesin-13-induced depolymerization *in vitro*

(A) Polarity marked GMP-CPP-stabilized rhodamine-labeled microtubules were attached to the coverslip by an anti-rhodamine antibody. The minus end is closest to the region of higher fluorescence intensity in the microtubule. In the absence of Patronin, purified Kinesin-13 motor domain from P. falciparum (3 mM) depolymerizes both ends of the microtubule. In contrast, in the presence of GFP-Patronin (30 nM), Kinesin-13 only depolymerizes the dimmer, plus end (white arrows) while the minus end (yellow arrows) is stable. (Note: the higher concentration of Patronin precludes imaging of individual Patronins at microtubule ends as in Fig. 9). Scale bar, 10 μm. (B) Quantitation of Kinesin-13-induced depolymerization rates at the plus and minus ends (n = 30 microtubules for each condition; mean and SD). Data is representative of three independent experiments with different microtubule preparations. (C) Patronin was mixed with the indicated concentration of either full-length Kinesin-13 from hamster (C.g.) or the motor domain from P. falciparum (P.f.) and added to polarity marked microtubules. Minus ends that showed no detectable depolymerization by the time the plus end depolymerized by >50% of the microtubule length was scored as protected. Higher concentrations of the motors are able to compete with Patronin to depolymerize a subset of minus ends. Percentages are representative of two independent experiments.

Figure 11. GFP-Patronin protects microtubule minus ends from Kinesin-13-induced depolymerization *in vitro*

An alternative assay for measuring protection of microtubule minus ends by Patronin *in vitro*. (A) Purified Kinesin-13 motor domain (MCAK motor domain from P. falciparum; 4 μM) depolymerizes both ends of GMP-CPP-stabilized, rhodamine-labeled microtubules attached to the coverslip by an anti-tubulin antibody in the presence of 5 mM ATP. Different regions of fluorescence intensity in the microtubule provide markers for tracking the depolymerization of the two ends over time (arrows). Scale bar, 5 μm. (B) Here, microtubules are anchored at their minus ends to coverslip-absorbed Patronin (identical to Fig. 9B); free Patronin was removed by perfusion of the flow chamber. Addition of Kinesin-13 motor domain (as above) results in depolymerization of only the plus end. In this example, the left end of the microtubule is anchored to the Patronin-coated surface (note pivoting). Scale bar, 5 μm. (C) Quantitation of Kinesin-13-induced depolymerization rates at the plus and minus ends. For the control (no Patronin added), segmented microtubules were bound to kinesin and dynein coated surfaces and the direction of gliding during the Kinesin-13-mediated depolymerization reaction allowed the polarity to be determined (e.g. as in Figure 9D, 9E). For the Patronin assay, segmented microtubules were attached to surface-bound GFP-Patronin as shown in panel B. In Fig. 9C, we show that the anchored end is the minus end of the microtubule. The depolymerization rates of the plus and minus end are shown (n = 40 microtubules scored for each condition; mean and S.D.).

	Wildtype	Patronin RNAi
Microtubule Plus End		
Growth (μm/min)	3.58 ± 1.10	4.22 ± 1.31
Shrinkage (μm/min)	10.21 ± 2.12	10.93 ± 1.56
Catastrophe (min^{-1})	0.12 ± 0.06	0.11 ± 0.05
Rescue (min^{-1})	0.16 ± 0.08	0.21 ± 0.08
Microtubule Minus End		
Shrinkage I (μm/min)	0.01 ± 0.07*	3.93 ± 0.87
Shrinkage II (μm/min)	N.D.	10.20 ± 2.21

Table 1. Quantitation of dynamic instability parameters in wildtype and Patronin depleted GFP-tubulin cells. Polymerization and depolymerization rates were measured for 25 individual microtubules (per type of measurement) from 8-16 cells over 3 different experiments. The number reported is the mean and S.D. from the 25 measurements. Polymerization and depolymerization rates were measured by kymograph analysis using ImageJ. For Patronin RNAi cells, "free" microtubules were measured (both ends clearly visible). The exception (noted by an *) is the minus end dynamics in wildtype cells. Because of the high degree of stability and possible movement of the microtubule in the wildtype cytoplasm over long measurement times, we measured the microtubule minus end relative to a photobleach mark as in Fig. 3 (n = 10); the value shown is within the error of our measurement and indicates that the minus end is very stable. "N.D.", indicates that a second rate was not detected. A comparable measurement of a minus end relative to a bleach mark in Patronin RNAi cells yielded two shrinkage rates (3.21 ± 0.31 and 10.81 ± 0.94; n = 20 for each rate), similar to that observed for tracking the minus end in microtubules without photobleach marks (shown in the Table). The microtubules scored for this table exhibited a single, constant minus end shrinkage rate. However,

these two different rates of minus end shrinkage occasionally were observed for individual microtubules (Figure 2E). Catastrophe and rescue frequencies were calculated for 10 cells per condition. In each cell, 10 microtubules were observed and the frequency of catastrophe and rescue calculated over the course of 3 min. The number reported is the mean and S.D. of the frequencies calculated for each cell.

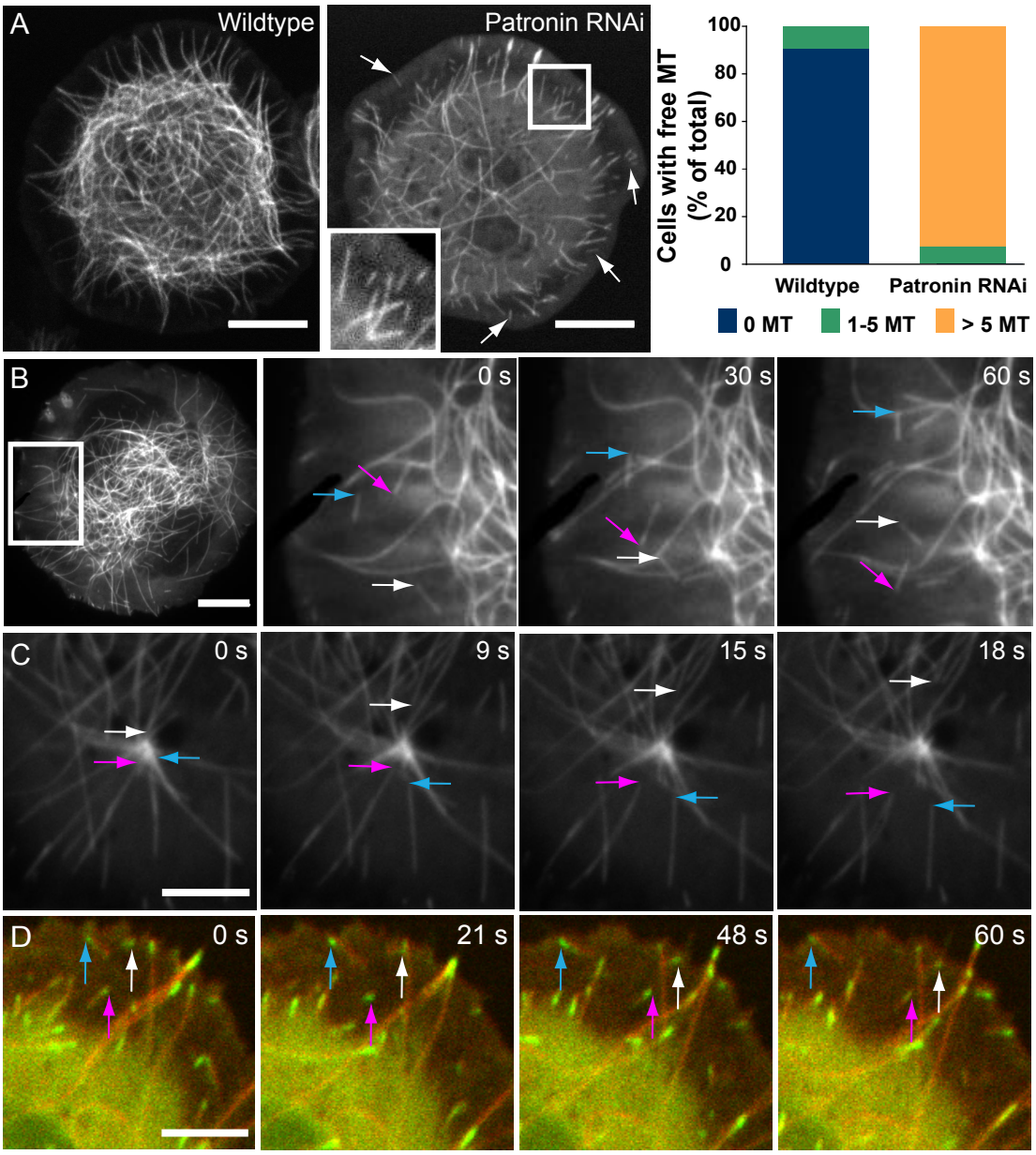
A
Wildtype
Patronin RNAi
Cells with free MT (% of total)
100
80
60
40
20
0
Wildtype
Patronin RNAi
0 MT
1-5 MT
> 5 MT
B
0 s
30 s
60 s
C
0 s
9 s
15 s
18 s
D
0 s
21 s
48 s
60 s

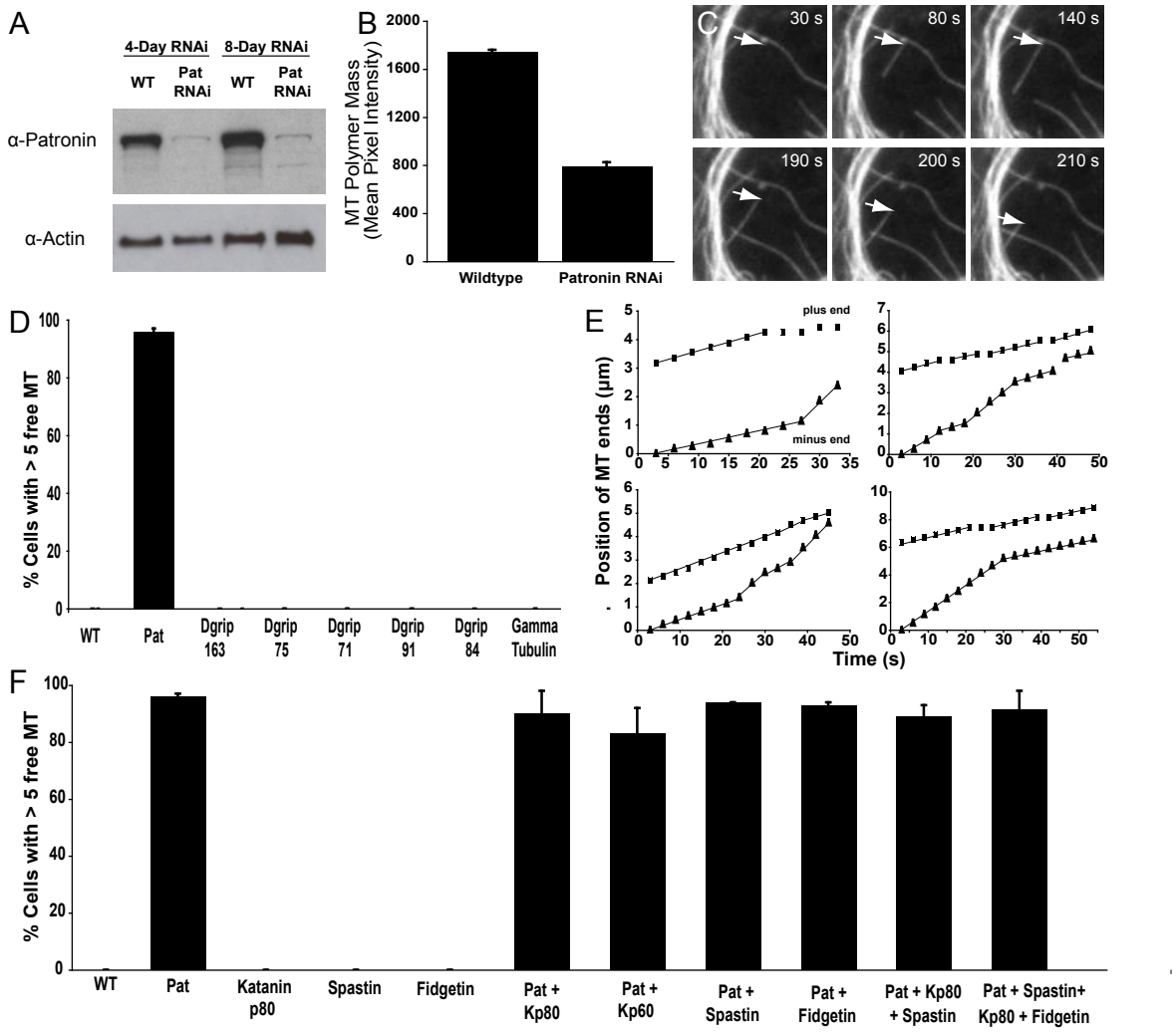
A
4-Day RNAi
8-Day RNAi
WT
Pat RNAi
WT
Pat RNAi
α-Patronin
α-Actin
B
MT Polymer Mass (Mean Pixel Intensity)
2000
1600
1200
800
400
0
Wildtype
Patronin RNAi
C
30 s
80 s
140 s
190 s
200 s
210 s
D
% Cells with > 5 free MT
100
80
60
40
20
0
WT
Pat
Dgrip 163
Dgrip 75
Dgrip 71
Dgrip 91
Dgrip 84
Gamma Tubulin
E
plus end
minus end
Position of MT ends (μm)
Time (s)
F
% Cells with > 5 free MT
WT
Pat
Katanin p80
Spastin
Fidgetin
Pat + Kp80
Pat + Kp60
Pat + Spastin
Pat + Fidgetin
Pat + Kp80 + Spastin
Pat + Spastin+ Kp80 + Fidgetin

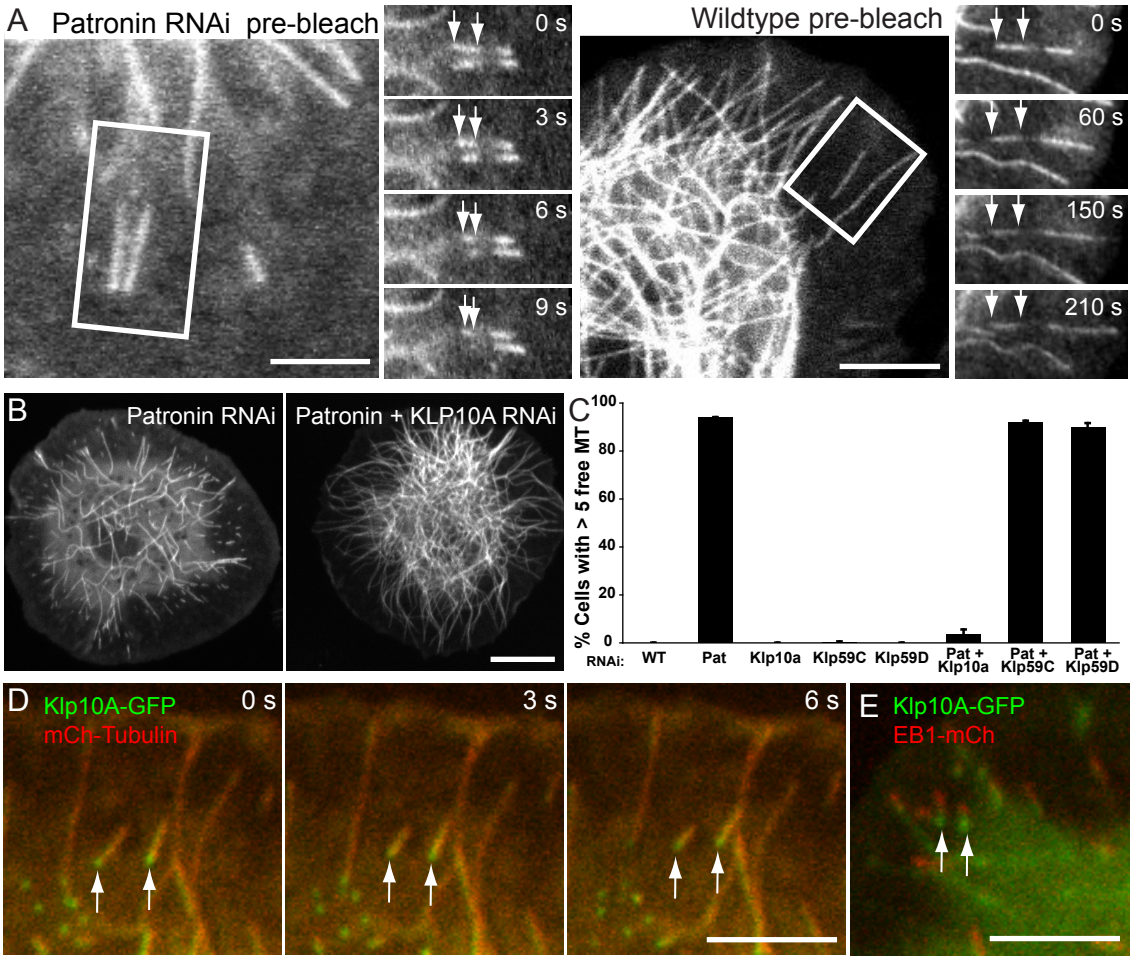
A
Patronin RNAi pre-bleach
0 s
3 s
6 s
9 s
Wildtype pre-bleach
0 s
60 s
150 s
210 s
B
Patronin RNAi
Patronin + KLP10A RNAi
C
% Cells with > 5 free MT
100
80
60
40
20
0
RNAi:
WT
Pat
Klp10a
Klp59C
Klp59D
Pat + Klp10a
Pat + Klp59C
Pat + Klp59D
D
Klp10A-GFP
mCh-Tubulin
0 s
3 s
6 s
E
Klp10A-GFP
EB1-mCh

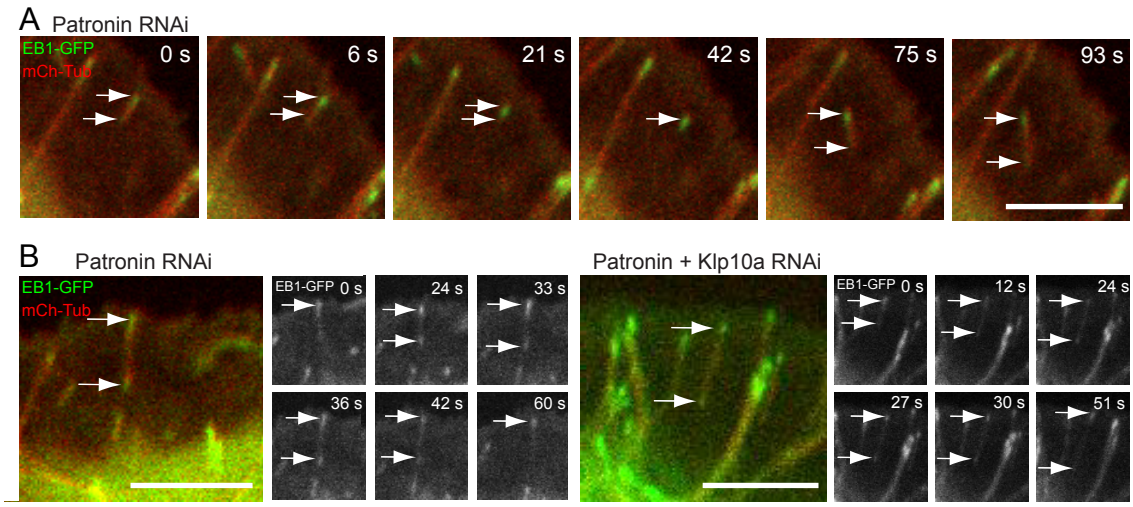
A
Patronin RNAi
EB1-GFP
mCh-Tub
0 s
6 s
21 s
42 s
75 s
93 s
B
Patronin RNAi
Patronin + Klp10a RNAi
EB1-GFP
mCh-Tub
EB1-GFP 0 s
24 s
33 s
36 s
42 s
60 s
EB1-GFP 0 s
12 s
24 s
27 s
30 s
51 s

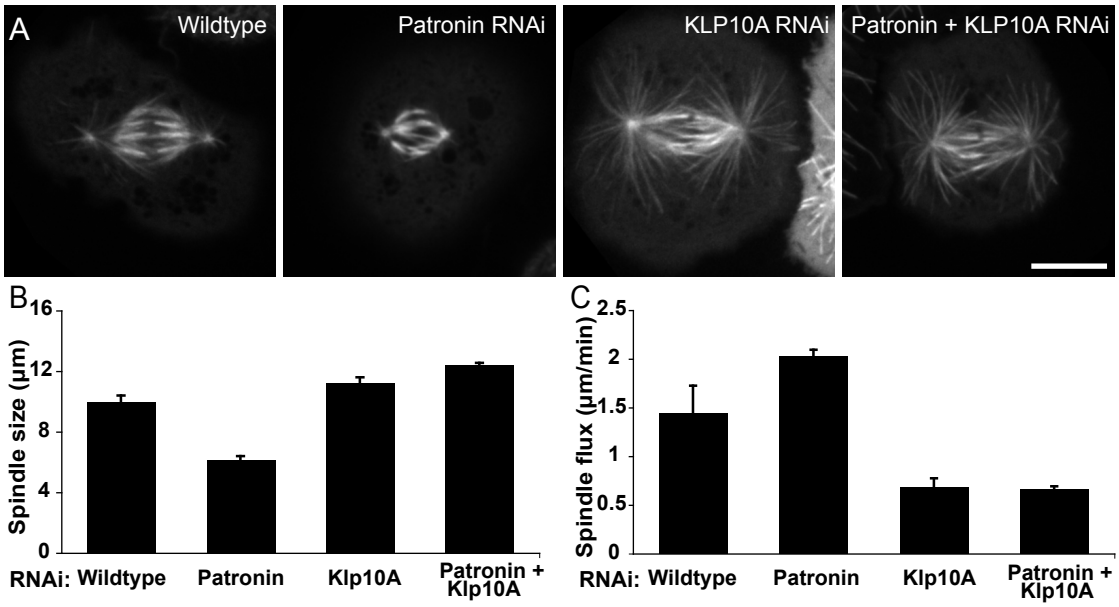
A
Wildtype
Patronin RNAi
KLP10A RNAi
Patronin + KLP10A RNAi
B
Spindle size (µm)
16
12
8
4
0
RNAi: Wildtype
Patronin
Klp10A
Patronin + Klp10A
C
Spindle flux (µm/min)
2.5
2
1.5
1
0.5
0
RNAi: Wildtype
Patronin
Klp10A
Patronin + Klp10A

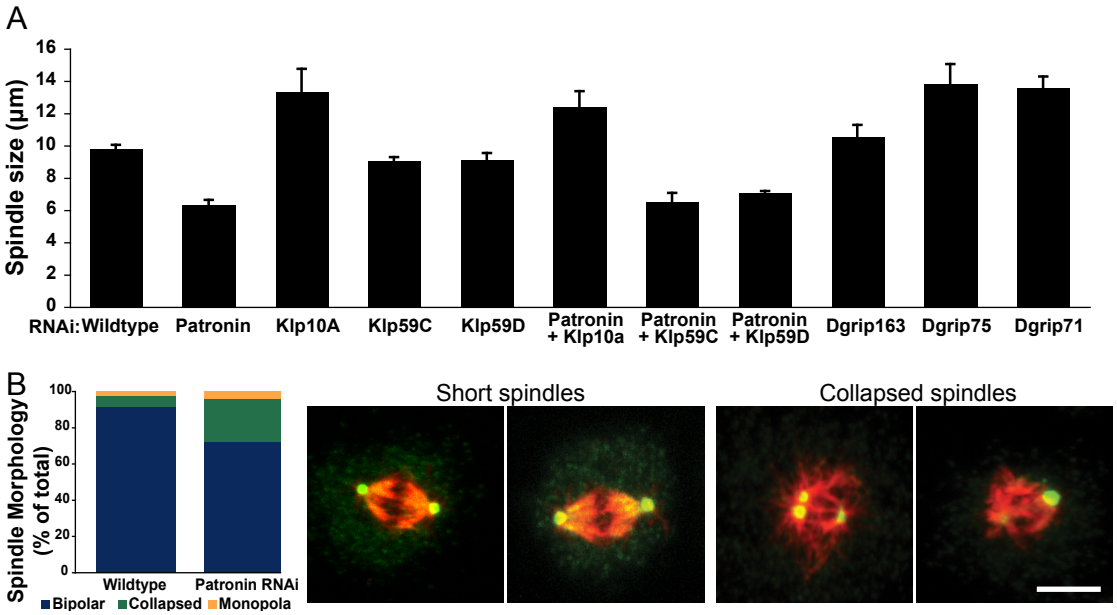
A
Spindle size (µm)
16
14
12
10
8
6
4
2
0
RNAi: Wildtype
Patronin
Klp10A
Klp59C
Klp59D
Patronin + Klp10a
Patronin + Klp59C
Patronin + Klp59D
Dgrip163
Dgrip75
Dgrip71
B
Spindle Morphology (% of total)
100
80
60
40
20
0
Wildtype
Patronin RNAi
Bipolar
Collapsed
Monopola
Short spindles
Collapsed spindles

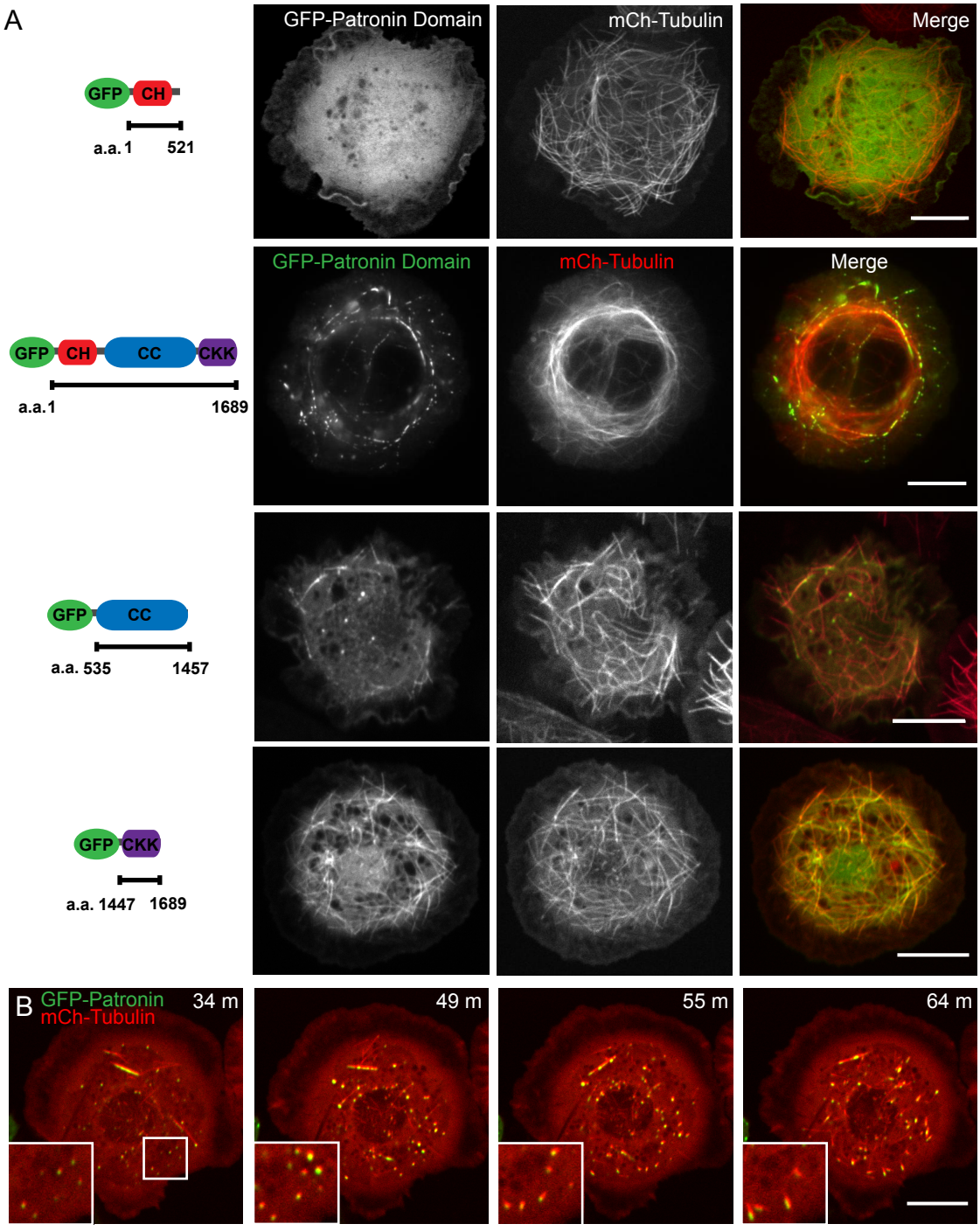
A
GFP
CH
a.a. 1
521
GFP-Patronin Domain
mCh-Tubulin
Merge
GFP
CH
CC
CKK
a.a.1
1689
GFP-Patronin Domain
mCh-Tubulin
Merge
GFP
CC
a.a. 535
1457
GFP
CKK
a.a. 1447
1689
B
GFP-Patronin
mCh-Tubulin
34 m
49 m
55 m
64 m

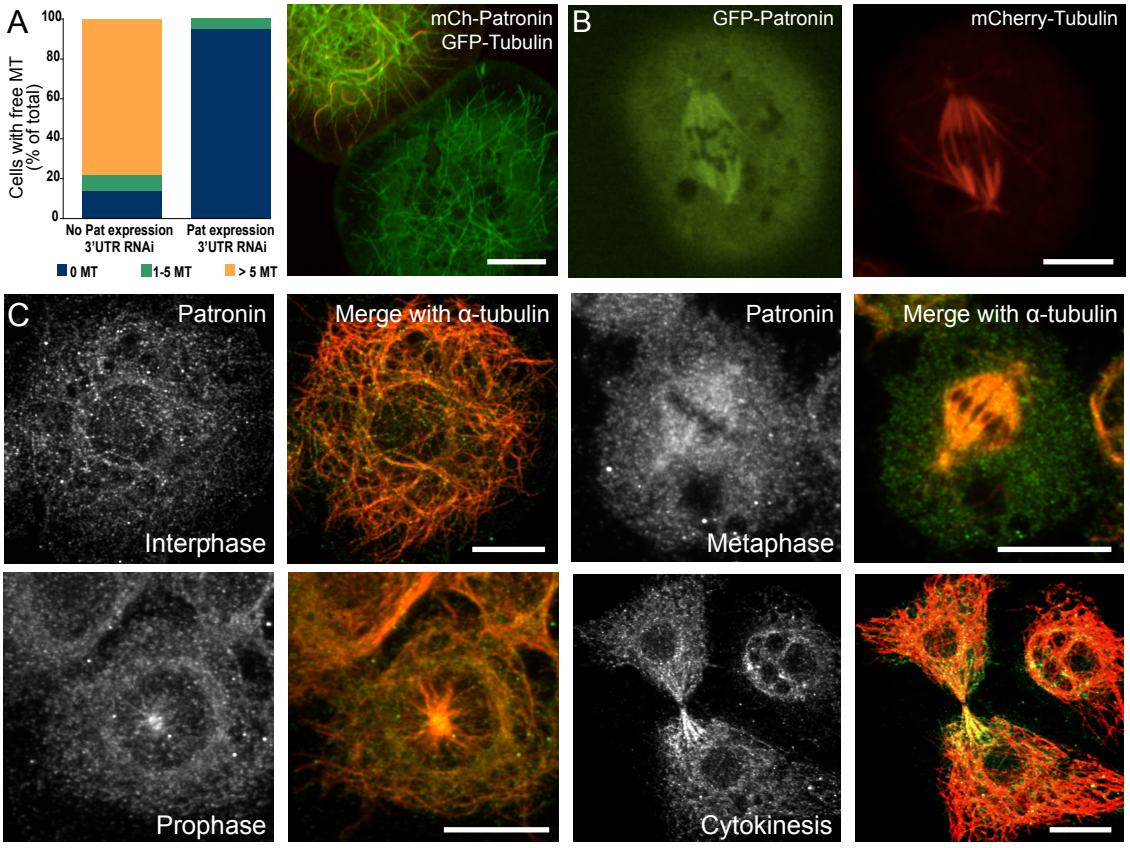
A
Cells with free MT (% of total)
100
80
60
40
20
0
No Pat expression 3'UTR RNAi
Pat expression 3'UTR RNAi
0 MT
1-5 MT
> 5 MT
mCh-Patronin
GFP-Tubulin
B
GFP-Patronin
mCherry-Tubulin
C
Patronin
Interphase
Merge with α-tubulin
Patronin
Metaphase
Merge with α-tubulin
Prophase
Cytokinesis

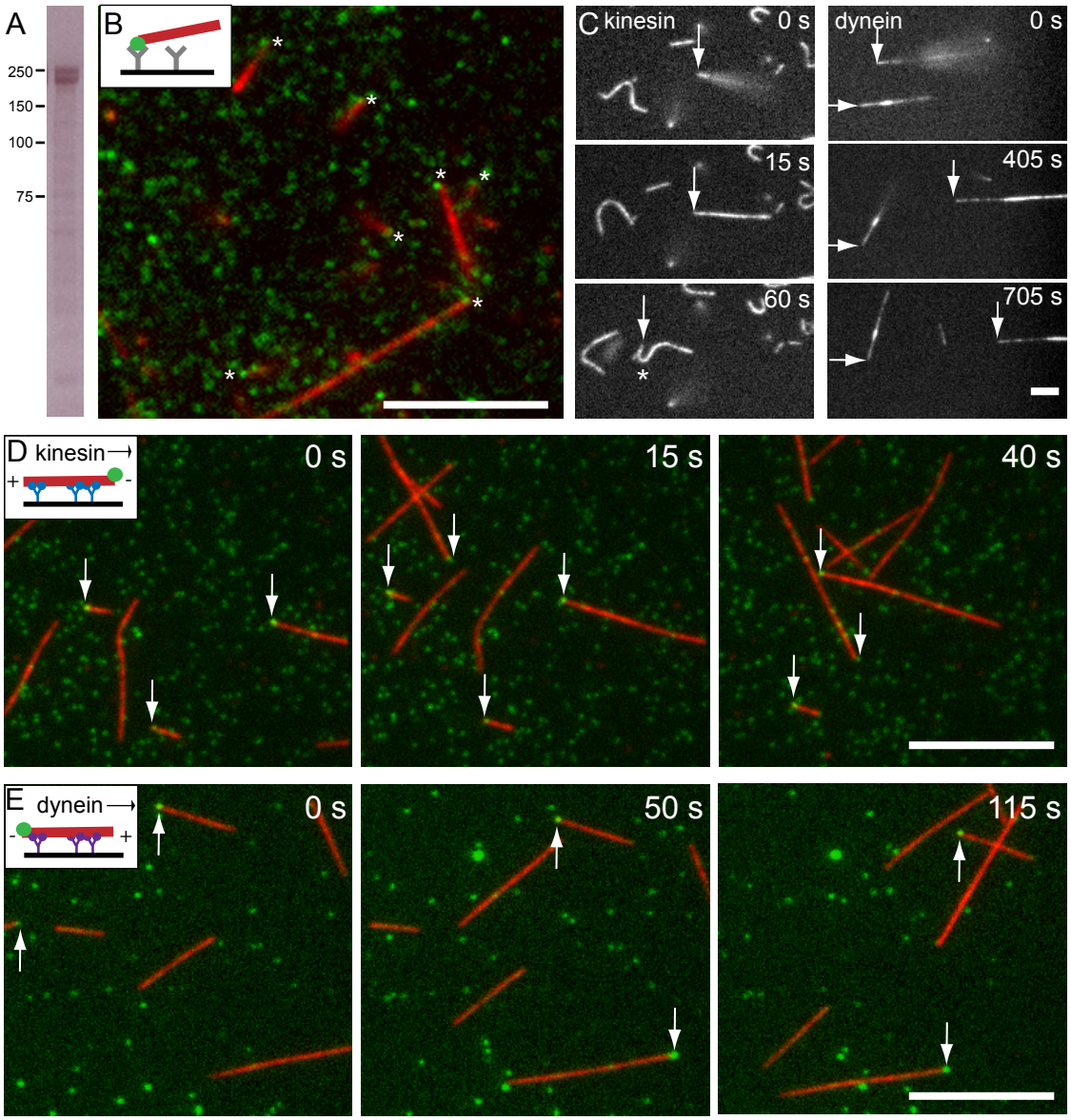
A
250
150
100
75
B
C kinesin
0 s
15 s
60 s
dynein
0 s
405 s
705 s
D kinesin
+
-
0 s
15 s
40 s
E dynein
-
+
0 s
50 s
115 s

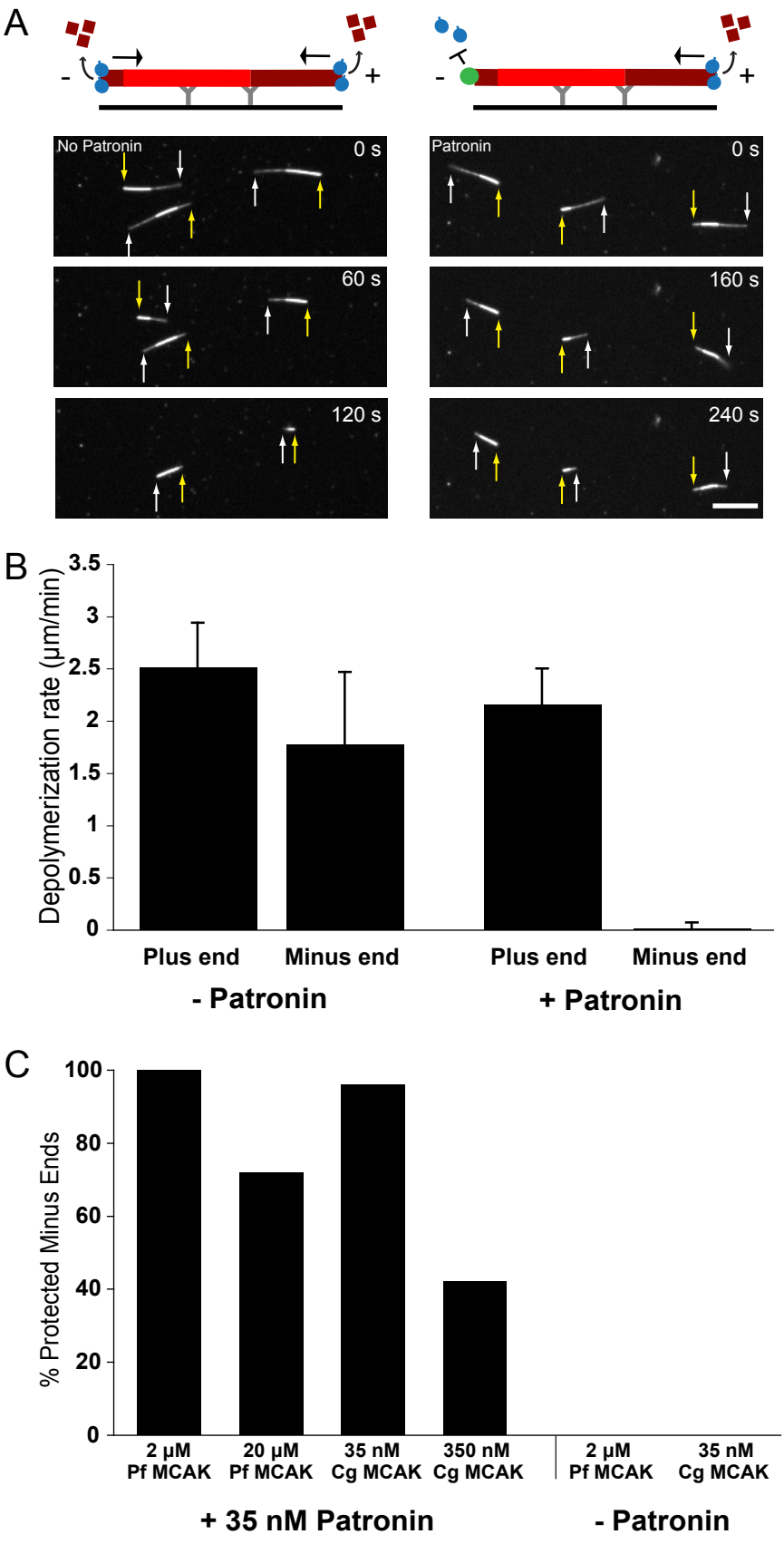
A
No Patronin
0 s
60 s
120 s
Patronin
0 s
160 s
240 s
B
Depolymerization rate (µm/min)
3.5
3
2.5
2
1.5
1
0.5
0
Plus end
Minus end
Plus end
Minus end
- Patronin
+ Patronin
C
% Protected Minus Ends
100
80
60
40
20
0
2 µM Pf MCAK
20 µM Pf MCAK
35 nM Cg MCAK
350 nM Cg MCAK
2 µM Pf MCAK
35 nM Cg MCAK
+ 35 nM Patronin
- Patronin

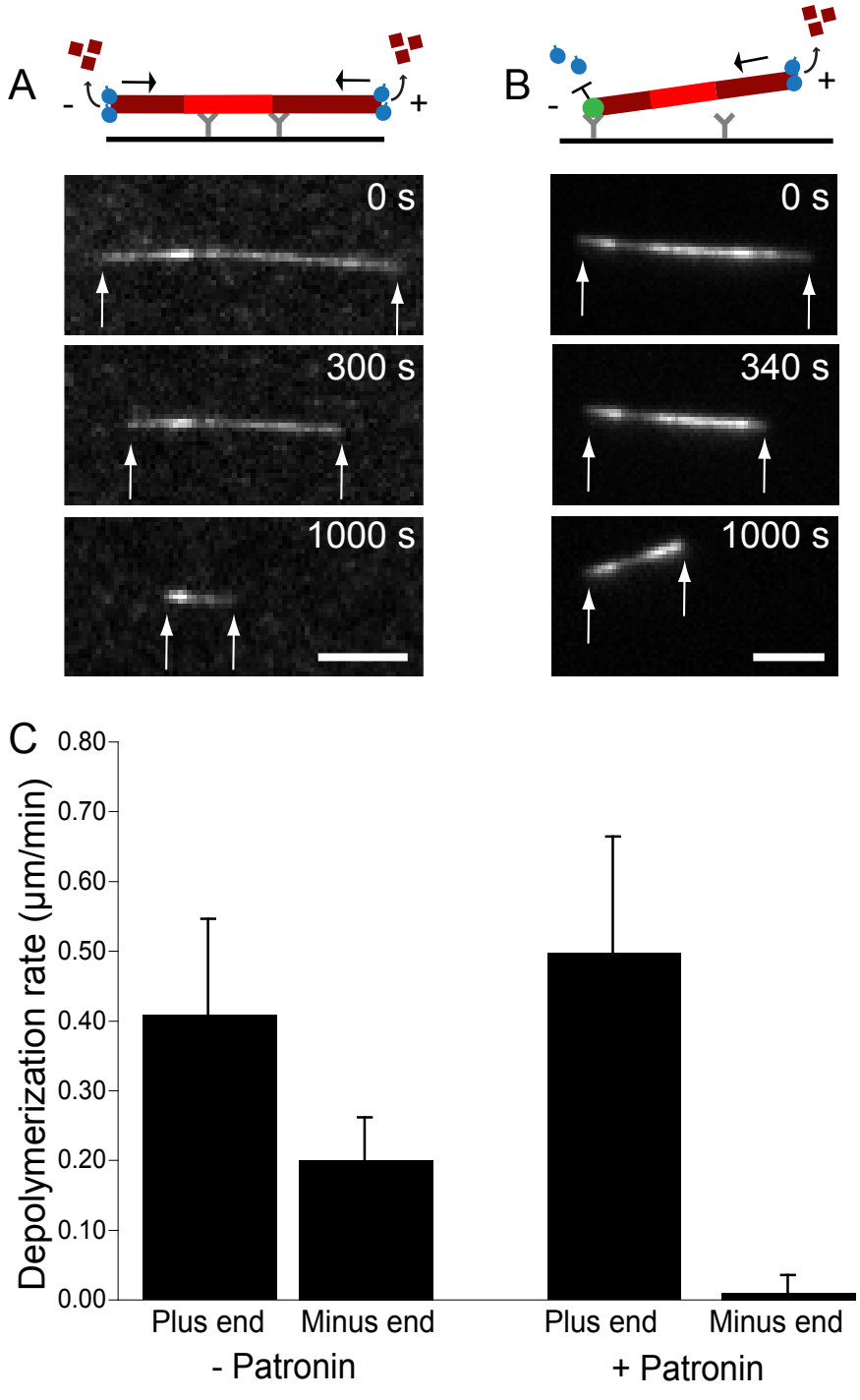
A
B
-
+
0 s
300 s
1000 s
340 s
C
Depolymerization rate (µm/min)
0.80
0.70
0.60
0.50
0.40
0.30
0.20
0.10
0.00
Plus end
Minus end
Plus end
Minus end
- Patronin
+ Patronin

Chapter 2

Patronin interacts with centrosomal proteins through its coiled-coil domain

Introduction

Cells have the ability to form a wide variety of highly organized microtubule arrays and therefore must have control over microtubule nucleation and organization. Some cell types have a microtubule organizing center (MTOC) or centrosome, which serves as the primary source of new microtubules as well as an organizational center for anchoring microtubules (Bettencourt-Dias and Glover, 2007). Centrosomes are composed of a large number of proteins (Hughes et al., 2008), many of which are highly conserved. The primary scaffold of the centrosome is the centriole, which has a 9-fold symmetry composed of the coiled-coil protein Sas-6 (Kitagawa et al., 2011; van Breugel et al., 2011). Although other structural details of the centrosome architecture remain to be solved, it is known that Sas-4 is involved in controlling the amount of pericentriolar material (PCM), the group of proteins including γ-tubulin that are responsible for directly promoting microtubule nucleation, which are recruited to the centriole (Kirkham et al., 2003). Another important protein is the kinase, SAK, which is necessary for regulating centriole duplication and centrosome formation (O'Connell et al., 2001; Peel et al., 2007).

Although the centrosome is essential in certain cell types, there are a wide variety of cells that do not rely on a centrosome for nucleation, organization, or both. These include cells in fungi, plants, flies, and many differentiated mammalian cell types such as myotubes, neurons, and epithelial cells (Bartolini and Gundersen, 2006; Rogers et al., 2008). Plants are particularly interesting as they do not have centrosomes at all. Instead microtubules are nucleated by small cortical nucleation centers and new microtubules are organized along the pre-existing microtubule array (Ehrhardt, 2008). The details of this process are currently being elucidated. Until recently it was thought that microtubules in neuronal and epithelial cells nucleated from a centrosome, released from the nucleation site, migrated and became anchored to discrete sites throughout the cytoplasm. However, a recent study demonstrated that neurons do not need centrosomes for axon elongation and regeneration and instead these processes occur through yet to be identified non-centrosomal pathways (Stiess et al., 2010). Although a role for non-centrosomal nucleation has not yet been determined for epithelial cells, these cells have apical microtubules that grow from foci containing the human Patronin homolog, Nezha, suggesting that microtubules originating from the centrosome migrate there, or that other pathways for microtubule nucleation may exist (Meng et al., 2008).

Drosophila provide a unique model system in which to study the formation of non-centrosomal microtubule arrays. Although Drosophila use centrosomes to nucleate and organize microtubules during mitosis, these centrosomes break down and disappear during interphase (Rusan and Rogers, 2009). Intriguingly, γ-tubulin and γ-TuRC are not necessary for interphase microtubule organization (Rogers et al., 2008; Bouissou et al.,

2009), suggesting there are unidentified pathways involved in microtubule array formation.

There are several lines of evidence that Patronin localizes to sites of new microtubule nucleation and is essential for non-centrosomal microtubule organization in Drosophila S2 cells. In Chapter 1, I demonstrated that Patronin is the major microtubule minus end stabilizer in Drosophila S2 cells. During my studies, I noticed that free microtubules were nucleated and released from small puncta containing α-tubulin in the absence of Patronin, suggesting Patronin might normally function at these puncta. These small puncta were visible in wildtype cells, but were more difficult to see due to the density of the microtubule array. Furthermore I observed microtubules growing out of GFP-Patronin puncta during a colcemid regrowth assay. If Patronin is broken down into domains and tagged with a fluorescent marker, the coiled-coil domain localizes to puncta in addition to short segments of a few microtubules. In cells expressing GFP-Patronin coiled-coil domain that are depleted of endogenous Patronin, microtubules can be seen growing from and treadmilling away from GFP-Patronin coiled-coil containing puncta (GFP-Patronin coiled-coil does not rescue the Patronin phenotype).

These lines of evidence suggest that Patronin localizes to sites of microtubule nucleation. Therefore we wanted to see if we could identify Patronin interacting proteins to uncover other proteins needed for microtubule nucleation and organization. These proteins have the potential to provide great insight into how non-centrosomal microtubule arrays are formed in a variety of cell types and organisms.

Results

Patronin coils have distinct localizations

The Patronin coiled-coil domain (referred to in this chapter as PatC1C2C3) has three predicted coiled-coils (Figure 1A)(Lupas et al., 1991). When the entire coiled-coil domain is expressed and tagged with GFP, it localizes to puncta and along small stretches of microtubules (Figure 1A). To determine if the coiled-coils are responsible for interacting with specific proteins, we made Patronin constructs expressing each coil on its own or expressing combinations of coils. When GFP-tagged first coil, second coil, or the first and second coil constructs were expressed, the localization was diffuse (data not shown). This suggests these coils do not have distinct localization patterns or that the truncated protein is unstable. To distinguish between these possibilities, more truncations should be made that include a greater number of amino acids in order to increase the chances the protein will be stable.

When a GFP-labeled construct containing both the second and third coil (PatC2C3) was expressed, the localization resembled that of the full-length coiled-coil domain (Figure 1B). Interestingly, when the GFP-labeled third coil of Patronin (PatC3) was expressed, it localized to puncta throughout the cell (Figure 1C). These puncta were reminiscent of foci observed with fluorescently tagged centrosomal proteins. For comparison, we made a construct containing the third coil plus the microtubule binding

CKK domain (see Chapter 1). This construct now localized to all microtubules (Figure 1D). When the entire coiled-coil domain and CKK domain was labeled with GFP and expressed, the construct localized to a subset of microtubules, reminiscent of full-length GFP-Patronin localization (Figure 1E).

Taken together, GFP-PatC1C2C3 and GFP-PatC2C3 have similar localizations, but GFP-PatC3 is dramatically different, suggesting that the second coil is responsible for binding to microtubules either directly or indirectly. Meanwhile the third coil is responsible for localizing Patronin to puncta reminiscent of nucleation centers. It is interesting that inclusion of the CKK domain results in localization along all microtubules, instead of in puncta, while the entire coiled-coil plus CKK domain localizes to a subset of microtubules. This data also suggests some direct or indirect interaction with microtubules in the second coil.

GFP-Patronin can recruit centrosomal proteins *in vivo*

Since Patronin localized to punctate sites of new microtubule nucleation during the microtubule regrowth assay, and PatC3-GFP localized to similar looking puncta, we wanted to determine if Patronin would co-localize with any known centriolar/centrosomal markers. GFP-Sas-4 and SAK are normally distributed as discrete cytoplasmic puncta (Figure 2A, 2C). However, when full-length mCherry-Patronin was overexpressed along with Sas-4 and SAK, these proteins were dramatically recruited to Patronin microtubules (Figure 2B, 2D). Meanwhile, Sas-6, Ana-1, Ana2, Ana-3, Dgt-2, Dgt-4, Dgt-5, Dgt-6,

Dgrip-193, Dgrip-71, and Cnn did not co-localize with Patronin (Figure 2E, 2F, and data not shown). Thus, Patronin may directly or indirectly interact with a subset of proteins associated with microtubule nucleating centers.

To determine which domain of Patronin interacts with Sas-4 and SAK, we co-expressed either the full-length coiled-coil domain (PatC1C2C3) or the microtubule binding (CKK) domain with fluorescently tagged Sas-4 or SAK. When mCherry-CKK domain was expressed with either GFP-Sas4 or GFP-SAK, there was no clear co-localization between these proteins (Figure 3A). Meanwhile, when the mCherry-PatC1C2C3 domain was co-expressed with either GFP-Sas-4 or GFP-SAK, GFP-Sas-4 and GFP-SAK co-localized with the GFP-PatC1C2C3 domain in puncta and along microtubules (Figure 3B), suggesting this domain is responsible for the interaction of SAK and Sas-4 with full-length Patronin.

To determine a minimal Patronin domain necessary for this interaction, we co-expressed Sas-4 with Patronin coiled-coil truncations. When mCherry-PatC2C3 was co-expressed with GFP-Sas-4, Sas-4 was recruited to puncta and along microtubules, co-localizing with PatC2C3 (Figure 3C). When only the third coil, PatC3-GFP, was co-expressed with mCherry-Sas-4, both proteins completely co-localized to puncta throughout the cytoplasm (Figure 3D). Taken all together, these results implicate the third coiled-coil as being important for interacting with Sas-4 and/or other microtubule nucleating proteins.

Patronin may interact with the scaffolding protein Asterless *in vivo*

Recently, several groups demonstrated that a centrosomal protein named Asterless could directly interact with Sas-4 and SAK (Varmark et al., 2007; Cizmecioglu et al., 2010; Hatch et al., 2010). Therefore we hypothesized that Patronin might also interact with Asterless, which in turn could scaffold Sas-4 and SAK. As previously reported, GFP-Asterless localizes to discrete puncta distributed throughout the cytoplasm (Figure 4A). These puncta co-localized to some, but not all mCherry-Sas4 puncta (Figure 4B), suggesting that upon Sas-4 over-expression, not all the cytoplasmic puncta have the same protein composition. Strikingly, when full-length GFP-Patronin was co-expressed with mCherry-Asterless, Asterless was recruited to Patronin microtubules, similar to Sas-4 and SAK (Figure 4C).

We next wanted to determine which domain was responsible for the Asterless interaction. When GFP-PatC1C2C3 was co-expressed with mCherry-Asterless, Asterless no longer strongly co-localized with Patronin on microtubules, and instead formed larger aggregates of variable size that also contained GFP-PatC1C2C3 (Figure 5B). Meanwhile, GFP-PatC2C3 did not strongly co-localize with mCherry-Asterless aggregates (Figure 4D). Similar to Sas-4, PatC3-GFP co-localized with some, but not all mCherry-Asterless puncta (Figure 4E), suggesting the third coil does not directly interact with Asterless. Taken together, these results indicate that amino acid residues in the first coil of Patronin

are responsible for the interaction with Asterless. Interestingly, Sas-4 and Patronin share a small stretch of similar amino acids:

```
Patronin 535 RMKLEEKRRRIEQDKR  544
             RMK+EE+RR+ EQ  R
Sas4     500 RMKIEEERRKFEQQMR  515
```

This sequence is located in the first coil of Patronin and is also found in the region of Sas-4 that interacts with Asterless (Dzhindzhev et al., 2010). We made two E→K and three R→E mutations in this coil to disrupt charge and therefore potential protein-protein interactions, while keeping the structure of the coil intact (Figure 5A). The localization of this mutant (GFP-PatC1C2C3mutant) was the same as the wild-type coiled-coil construct (data not shown). When GFP-PatC1C2C3mutant was co-expressed with mCherry-Asterless, the proteins still co-localized into puncta, however the puncta often appeared smaller. (Figure 5B and 5C). These results suggest that the RMKLEEKRRRIEQDKR sequence may play a role in Patronin's interaction with Asterless, however it is not the only interaction site. Another interaction may be mediated through the third coil (PatC3), which co-localizes with a subset of the Asterless puncta (Figure 4E). Another possibility is that the charge reversal was not sufficient to disrupt the interaction, and that a change to hydrophobic residues may cause a more dramatic difference.

Human Patronin localizes to microtubules in interphase and the spindle in mitosis

There are three human Patronin homologs, Camsap1 (Patronin 1), Camsap1L1 (Patronin 2), and Nezha (Patronin 3)(Baines et al., 2009). When GFP-Patronin 2 is expressed in HeLa cells, GFP-Patronin 2 binds to a subset of microtubules, the mitotic spindle, and the midbody, similar to the localization pattern of Drosophila Patronin (Figure 6A). As mentioned in Chapter 1, Patronin 3 localizes to microtubule minus ends in epithelial cells (Meng et al., 2008). Therefore is it highly likely that these human Patronins are indeed functional homologs of Drosophila Patronin.

Each human Patronin has a calponin homology (CH) domain at its N-terminus, three coils in the middle of the protein, and the CKK/Duf1781 microtubule binding domain at its C-terminus. As demonstrated for Drosophila Patronin, the coiled-coil mediates interactions with other proteins. Interestingly, the greatest variability between human Patronin isoforms is in the coiled-coil region (Baines et al., 2009), suggesting these isoforms may interact with different proteins. Indeed, Patronin 3 was identified because it interacted with PLEKHA7, a zonula adherens component in epithelial cells(Meng et al., 2008). Patronin 1 is specifically found in astrocytes, as opposed to other neuronal cells (Yamamoto et al., 2009) suggesting these isoforms may also be expressed in specific cell types.

We used sequence alignments to compare the potential Asterless-interaction region in Drosophila Patronin with the same region in the three human isoforms to see if there are conserved residues in this area. Patronin 2 has the highest conservation in this region with Drosophila Patronin (Figure 6B). This information, along with the similar cellular localizations of these two proteins, suggest Patronin 2 may be the closest related protein to Drosophila Patronin, while the other two isoforms may have evolved to interact with other proteins or express in specific cell types. Further studies of human Patronins, including depletion studies in interphase and mitosis, as well as truncation analysis will be necessary to further test this hypothesis.

Discussion

The *in vivo* co-localization studies of Patronin strongly suggest a role in scaffolding centrosome proteins. Full-length Patronin co-localizes with Sas-4, SAK, and Asterless, recruiting these proteins to Patronin microtubules. While the coiled-coil domain (PatC1C2C3) also co-localizes with these three proteins, Sas-4 and SAK are recruited to Patronin microtubules, while Asterless forms aggregates containing Patronin. This aggregate co-localization is lost when Asterless is expressed with PatC2C3. When Sas-4 is over-expressed, Sas-4 and PatC3 completely overlap in puncta, while PatC3 and Asterless only co-localize in a subset of puncta, implying that some of the 'extra' puncta found in Sas-4 overexpressed cells may not be true microtubule nucleating puncta. However, since Pat3 still localizes to these 'extra' puncta while Asterless does not, it suggests a more direct interaction between Patronin and Sas-4. Taken together, these results suggest that the third coil of Patronin interacts with Sas-4, while residues in the first coil interact with Asterless.

We became interested in Asterless after learning it biochemically interacted with Sas-4 and SAK and served as a scaffold for these proteins *in vivo* (Dzhindzhev et al., 2010). We already knew Patronin recruited Sas-4 and SAK and shared sequence homology with Sas-4, so it seemed that an interaction between Patronin and Asterless would be likely. Our data demonstrates that full-length Patronin can recruit Asterless to microtubules, while the coiled-coil domain forms aggregates that co-localize with Asterless. However, when we mutated residues in Patronin's first coil to disrupt

Asterless interaction, there were still puncta containing Asterless and Patronin, although the aggregates often appeared smaller. Therefore different mutations or biochemical assays are needed to really determine if these residues are indeed responsible for this interaction.

Patronin's coiled-coil region is very interesting. When all three coils are expressed (PatC1C2C3) the localization to puncta and along a few microtubules is striking. I had previously demonstrated that these puncta nucleate microtubules, as seen when endogenous Patronin is depleted (data not shown), however the localization along microtubules remains a mystery. Interestingly, constructs lacking Patronin's first coil maintain the microtubule/puncta localization however when only the third coil is expressed the microtubule binding is lost while the puncta localization remain. This strongly suggests that something in the second coil is responsible for Patronin's localization along a subset of microtubules. Whether this coil is mediating a protein-protein interaction, or an interaction with a particular modification of tubulin remains to be determined. Lastly, the third coil, which localizes to puncta and co-localizes with Sas-4 appears to be responsible for Patronin's localization to nucleation centers. It will be interesting to identify if Patronin is directly binding with Sas-4 or if it is binding to another centrosomal protein. In sum, Patronin's coils each appear to be responsible for a particular localization. The first coil is involved with binding to Asterless, the second coil is needed for binding a microtubule subset, and the third coil mediates binding to nucleation centers. This work provides a starting point for a more complete

understanding of Patronin's role in organizing the microtubule network beyond its protection function.

As discussed previously, Drosophila S2 cells do not have a central microtubule organizing center. Instead, upon microtubule depolymerization and regrowth, microtubules can be seen emanating from discrete areas throughout the cytoplasm (Rogers et al., 2008; Rusan and Rogers, 2009). The proteins involved in nucleating the microtubules from these locations remain to be determined, but it is known they do not include Sas-6, the canonical centriolar protein (Rogers et al., 2008). Patronin also does not co-localize with Sas-6, but it does co-localize with Sas-4, SAK, and Asterless, suggesting that the microtubule nucleation sites in Drosophila include a complex containing Patronin, Asterless, Sas-4, and SAK. As this data is all *in vivo*, biochemistry is necessary in future experiments to identify which proteins are interacting directly.

There is already evidence that the three human Patronin homologs are expressed in different cell types, but may have similar functional roles. Full characterization of the localization and depletion phenotypes of each homolog in interphase and mitosis, in addition to determining the *in vitro* activity is necessary to elucidate the conservation of Patronin between organisms. One appealing hypothesis is that each human Patronin isoform is expressed in specific cell types and its interaction partners via the coiled-coil region determine Patronin's cellular localization. Since every cell type has different nucleation and microtubule array patterns, this could be a way for the cell to ensure Patronin is localized to specific sites where microtubules need to be anchored, as well as

sites of new minus end formation. Supporting this hypothesis, the human Patronins have the most variation in the coiled-coil region and Patronin 2 localizes similarly to Drosophila Patronin (Figure 6A), while Patronin 3 localizes to specific sites near adherens junctions in epithelial cells (Meng et al., 2008). Further studies in a variety of human cells will elucidate the function of the three Patronin isoforms in forming different microtubule arrays.

Experimental Procedures

See experimental procedures in Chapter 1 for details on cell culture and live cell imaging.

Figure Legends

Figure 1. Patronin coils have different localizations

(A and B) Cells expressing the entire coiled-coil domain (GFP-PatC1C2C3) or the second and third coil (GFP-C2C3) localize to microtubules and puncta, while the third coil (GFP-PatC3) localizes to discrete puncta (C). When the third coil is expressed with the CKK domain (GFP-PatC3-CKK), Patronin localizes to al microtubules. The localization changes to a subset of microtubules when the entire coiled-coil plus CKK domain is expressed (GFP-PatC1C2C3-CKK). The likelihood that particular residues form coils, as predicted by the COILS program (Lupas et al., 1991), are shown to the right. Scale bars = 10 μm.

Figure 2. Patronin recruits SAK and Sas-4, but not Sas-6, to microtubules

(A) Cells expressing GFP-Sas-4 alone form cytoplasmic foci, but when GFP-Sas-4 is co-expressed with mCherry-Patronin (B), Sas-4 is recruited to sites of mCherry-Patronin along microtubules. (C and E) Cells expressing GFP-SAK or GFP-Sas-6. These proteins form cytoplasmic foci. (D and F) Cells expressing GFP-SAK or GFP-Sas-6 (green) along with high levels of mCherry-Patronin (red). Similar to GFP-Sas-4, GFP-SAK is now recruited to sites of mCherry-Patronin along microtubules, while GFP-Sas-6 does not co-localize with Patronin. Scale bars = 10 μm.

Figure 3. Patronin coiled-coil domains can recruit and co-localize with Sas-4.

(A) An mCherry fusion of Patronin's microtubule binding CKK domain (red) does not recruit and co-localize with GFP-Sas-4 (green). Meanwhile (B and C) mCherry-PatC1C2C3 (red) and mCherry-PatC2C3 (red) can recruit GFP-Sas-4 (green). (D) PatC3-GFP (green) and mCherry-Sas-4 (red) co-localize into cytoplasmic puncta. Scale bars = 10 μm.

Figure 4. Full-length Patronin recruits Asterless to microtubules

(A) GFP-Asterless localizes into discrete cytoplasmic puncta. (B) GFP-Asterless (green) co-localizes with a subset of mCherry-Sas-4 puncta (red). (C) GFP-tagged full-length Patronin (green) recruits mCherry-Asterless (red) to Patronin-labeled microtubules, while (D) GFP-PatC2C3 (green) and mCherry-Asterless (red) do not co-localize. (E) PatC3-GFP (green) and mCherry-Asterless (red) co-localize in a subset of the cytoplasmic puncta. Scale bars = 10 μm.

Figure 5. Patronin coiled-coil domain and Asterless co-localize into large aggregates

(A) Patronin and Sas-4 share sequence homology located in the first coil of Patronin. (B) To see if this sequence is responsible for Patronin's co-localization with Asterless, two E→K and three K→E mutations were made (arrows). (C) When wild type GFP-PatC1C2C3 (green) is co-expressed with mCherry-Asterless (red), large aggregates containing both Asterless and PatC1C2C3 form. (D) Meanwhile when GFP-PatC1C2C3mutant (green) is co-expressed with mCherry-Asterless (red), there is some co-localization in puncta but aggregates appear smaller in size. Scale bars = 10 μm.

Figure 6. Human Patronin 2 localizes to microtubules in interphase and mitosis

(A) GFP-Patronin 2 (Camsap1L1) expressed in HeLa cells localizes along microtubules in interphase and to the midbody, spindles, and centrosomes in mitosis. (B) Comparison of the potential Asterless-interaction region between Drosophila Patronin and the three Patronin isoforms showing that Patronin 2 has slightly higher conservation in this region than the other isoforms.

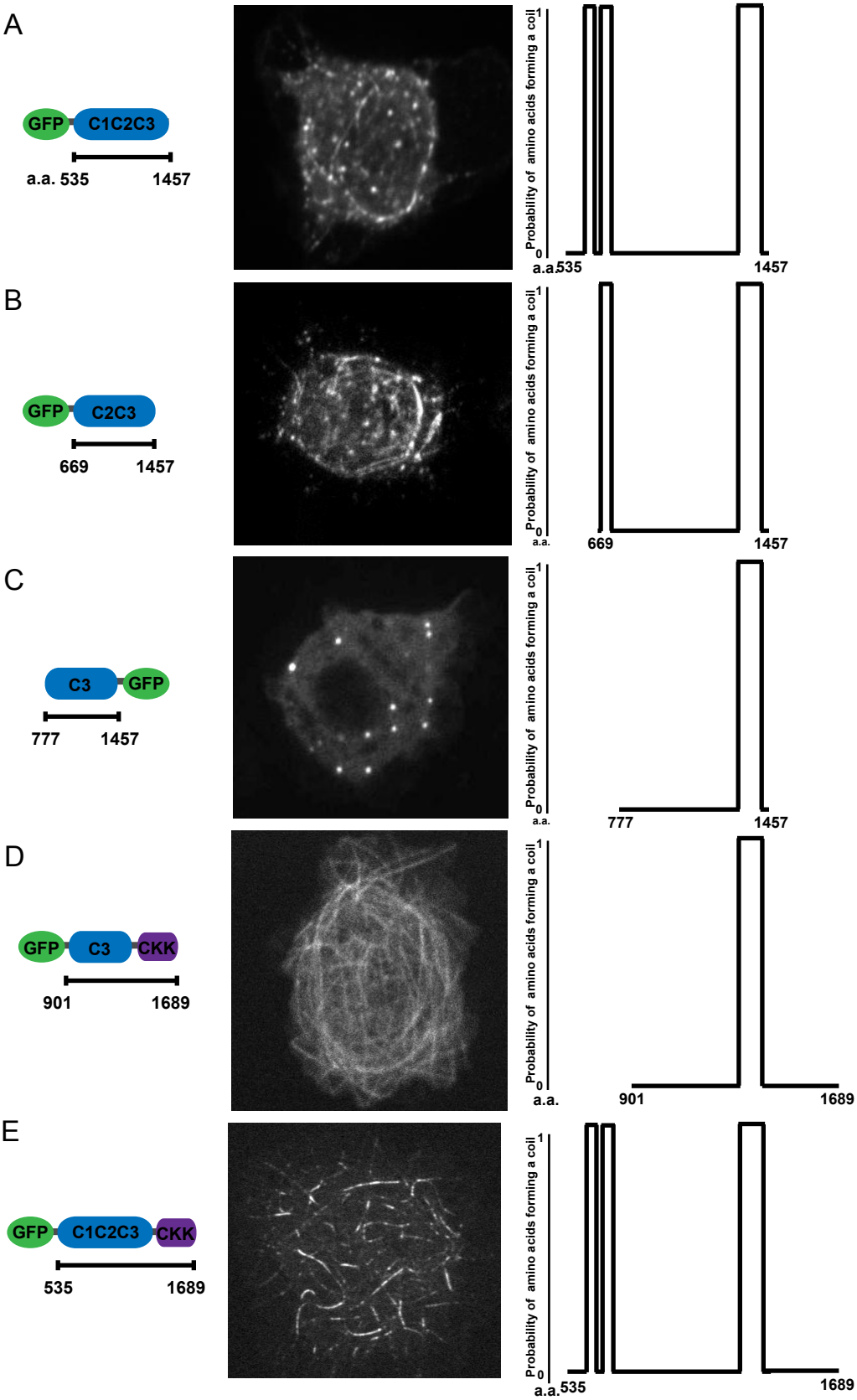
A
GFP
C1C2C3
a.a. 535
1457
Probability of amino acids forming a coil
1
0
a.a.
535
1457
B
GFP
C2C3
669
1457
Probability of amino acids forming a coil
1
0
a.a.
669
1457
C
C3
GFP
777
1457
Probability of amino acids forming a coil
1
0
a.a.
777
1457
D
GFP
C3
CKK
901
1689
Probability of amino acids forming a coil
1
0
a.a.
901
1689
E
GFP
C1C2C3
CKK
535
1689
Probability of amino acids forming a coil
1
0
a.a.
535
1689

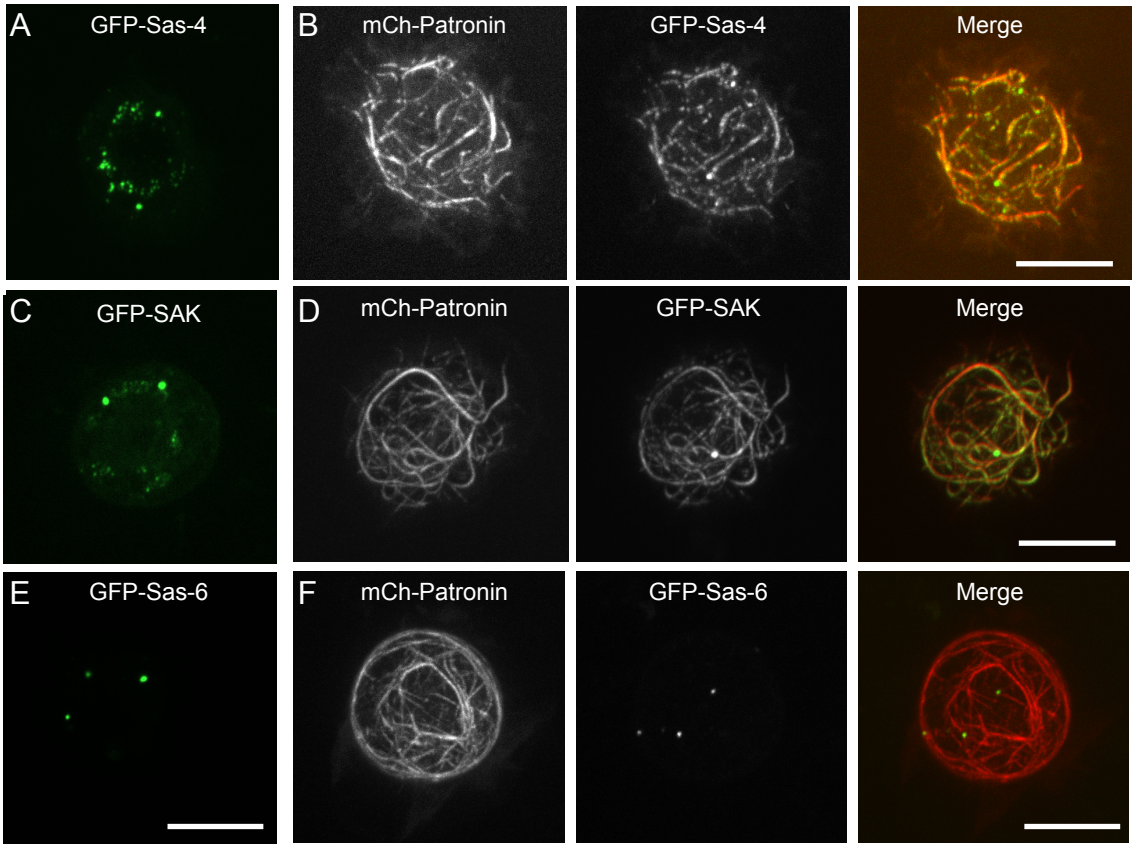
A
GFP-Sas-4
B
mCh-Patronin
GFP-Sas-4
Merge
C
GFP-SAK
D
mCh-Patronin
GFP-SAK
Merge
E
GFP-Sas-6
F
mCh-Patronin
GFP-Sas-6
Merge

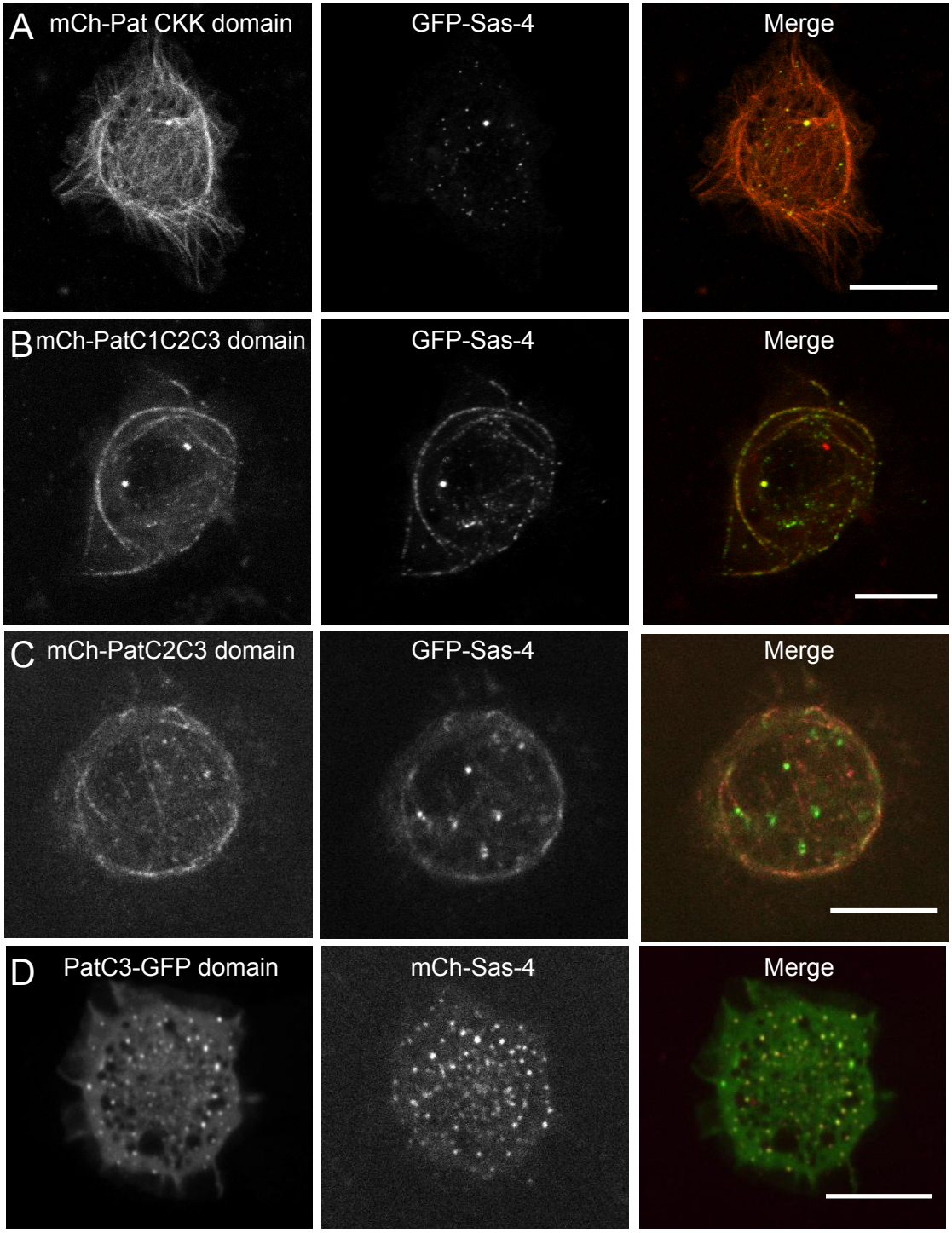
A
mCh-Pat CKK domain
GFP-Sas-4
Merge
B
mCh-PatC1C2C3 domain
GFP-Sas-4
Merge
C
mCh-PatC2C3 domain
GFP-Sas-4
Merge
D
PatC3-GFP domain
mCh-Sas-4
Merge

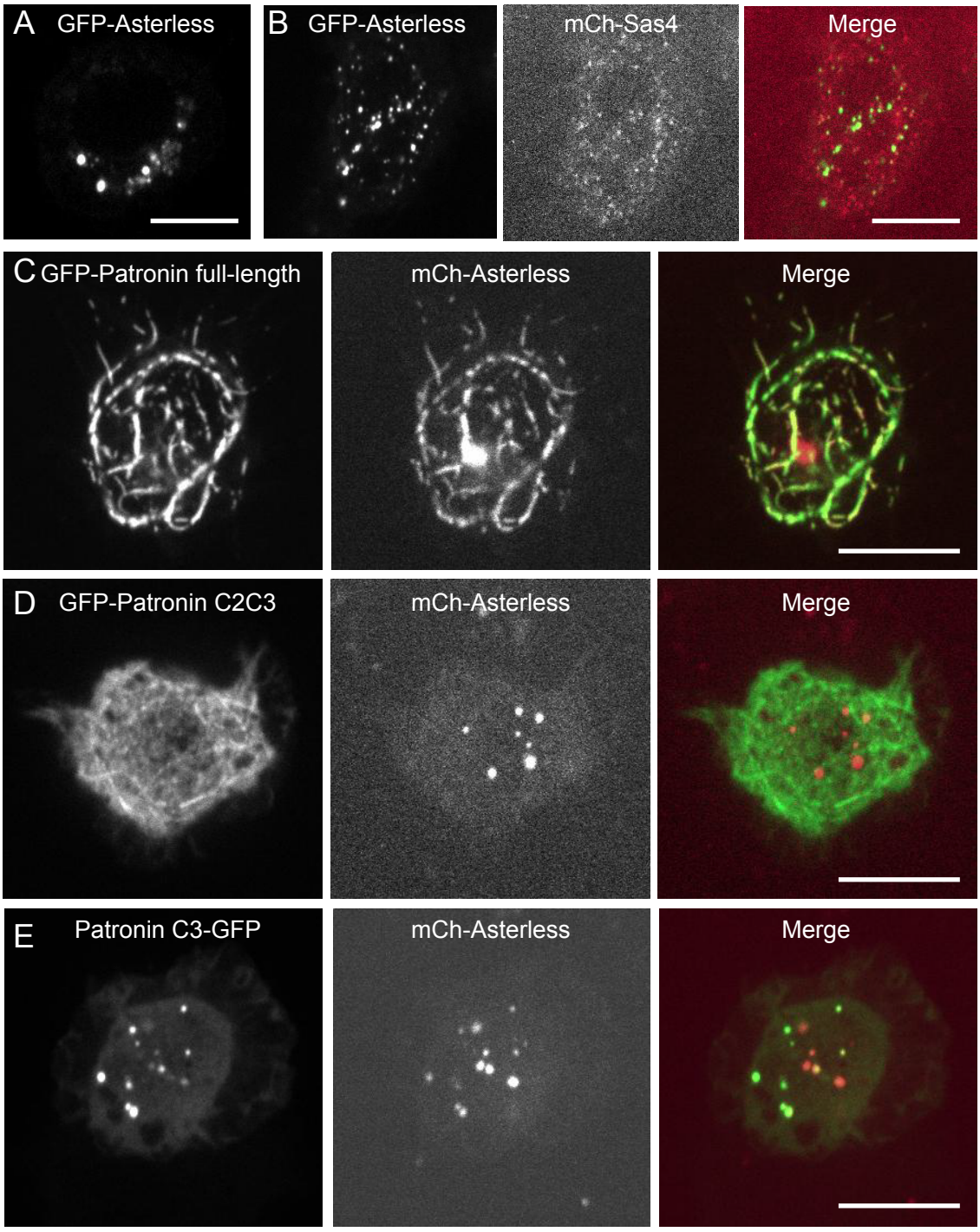
A GFP-Asterless
B GFP-Asterless
mCh-Sas4
Merge
C GFP-Patronin full-length
mCh-Asterless
Merge
D GFP-Patronin C2C3
mCh-Asterless
Merge
E Patronin C3-GFP
mCh-Asterless
Merge

A

```
Pat 535    RMKLEEKRRRIEQDKR  544
           RMK+EE+RR+ EQ  R
Sas4 500   RMKIEEERRKFEQQMR  515
```

B

```
Pat 535        RMKLEEKRRRIEQDKR  544
                   ↓↓ ↓ ↓↓
PatMutant 535  RMKLKKKEEEIEQDKR  544
```

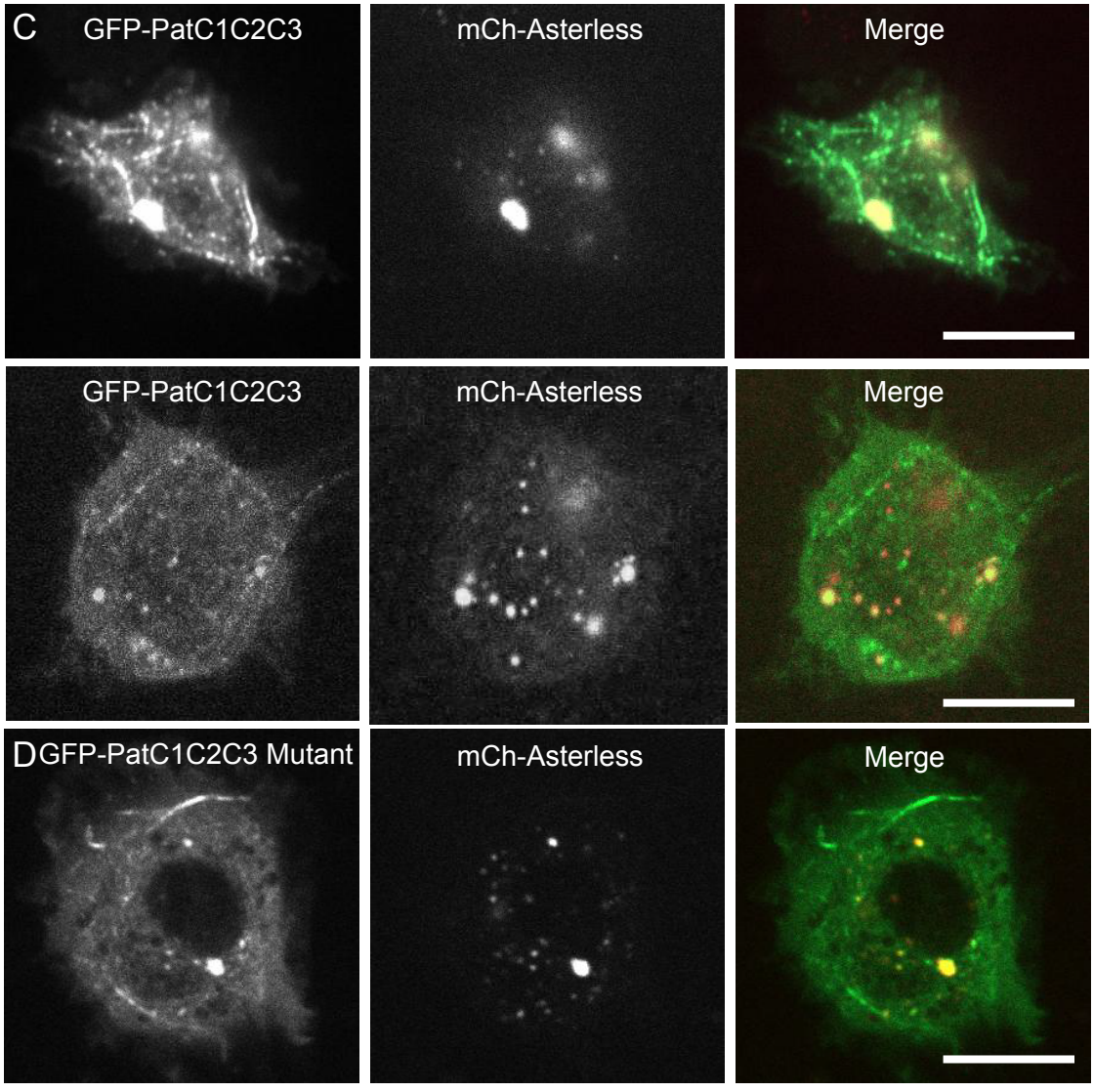

A

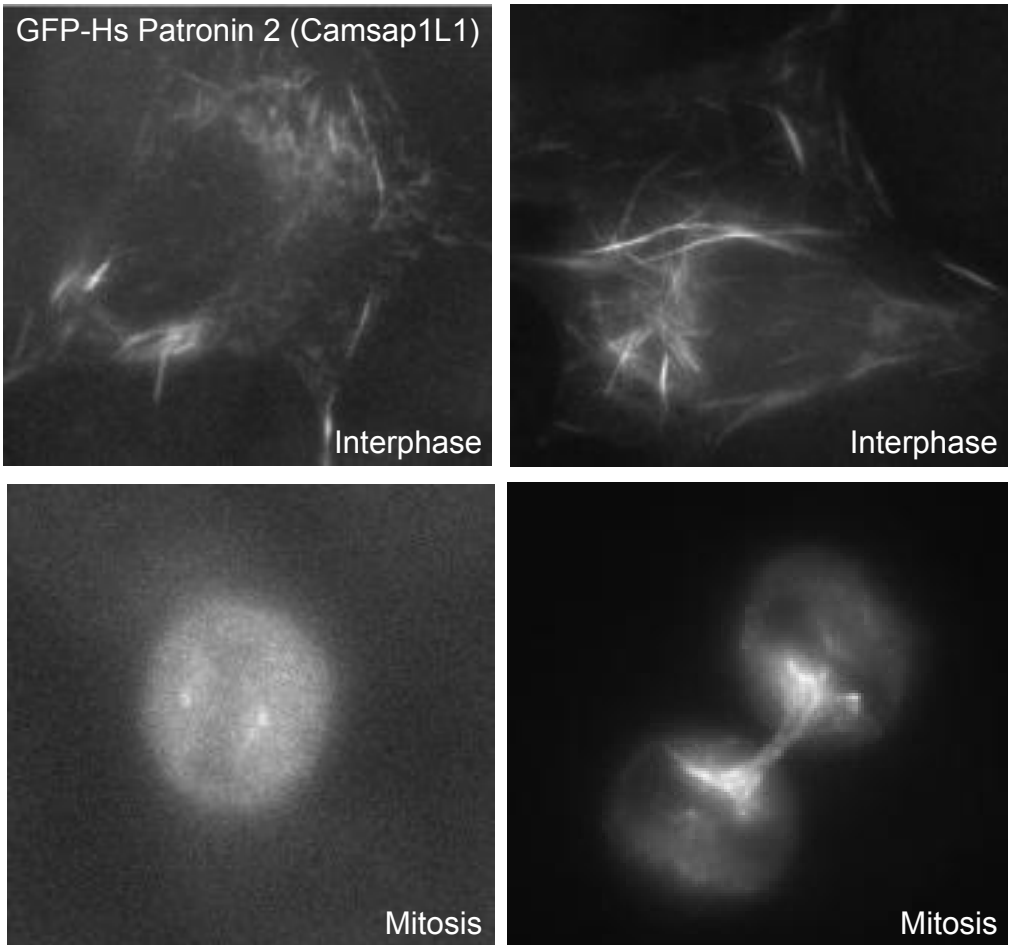

B

```
Dm Pat   624   ASKLSTIRMKLEEKRRRIEQDKRKIE   649
               AS+L  + M+LEEKRR IE  K+K+E
Hs Pat1  597   ASELVQLHMQLEEKRRAIEAQKKKME   622
(CS1)

Dm Pat   624   ASKLSTIRMKLEEKRRRIEQDKRKIE   649
               AS++  +RMKLEEKRR IE  K+K+E
Hs Pat2  747   ASEMVHLRMKLEEKRRAIEAQKKKME   772
(CSL1L)

Dm Pat   624   ASKLSTIRMKLEEKRRRIEQDKRKIE   649
               +S++S +  +LEEKRR IE  KR+IE
Hs Pat3  624   SSEMSELSARLEEKRRAIEAQKRRIE   649
(Nezha)
```

Conclusion

Expecto Patronin!

Microtubule minus ends exhibit dynamic instability *in vitro* but are mostly stable *in vivo*, a discrepancy that has remained a mystery for a long time. The identification and characterization of Patronin as a microtubule minus end capping protein has shed light on the regulation of the minus end. In the absence of Patronin, Klp10a binds to the minus end resulting in minus end depolymerization. In cells depleted of both Patronin and Klp10a, the minus end becomes a substrate for EB1. EB1 binding to the minus end is also observed in Patronin-depleted cells when minus end depolymerization pauses, presumably because Klp10a is momentarily unbound or inactive. Interestingly, both Klp10a and EB1 bind to both microtubule ends *in vitro*, suggesting both ends are suitable substrates for these proteins, and that perhaps they are not seen at minus ends *in vivo* because Patronin is preventing them from binding. This data is particularly exciting because it demonstrates that the minus end is subject to regulation by stabilizing, depolymerizing, and growth–promoting regulatory proteins and suggests there are yet to be identified proteins involved in regulating the minus end.

How does Patronin interact with the minus end? Do the two microtubule binding domains (CKK and the second coiled-coil) work together to clamp down on the microtubule end and physically stabilize the minus end or sterically hinder other proteins from binding? Or does Patronin bind in such a way that part of the protein is located inside the microtubule lumen? *In vitro*, Patronin selectively binds to the minus ends of

microtubules made from purified tubulin, suggesting it strongly recognizes the alpha tubulin residue facing the minus end, or some structure that is only accessible in the minus end conformation. Future structural and EM studies should help elucidate how Patronin interacts with minus ends.

Another unanswered question is how Patronin is regulated throughout the cell cycle. In interphase, most minus ends are stable, therefore Patronin protein levels and/or activity should be high. Meanwhile, in mitosis, minus ends need to be depolymerized in order to properly form a metaphase spindle and pull apart the chromosomes during anaphase, so Patronin protein levels and/or activity should be lower. Supporting this hypothesis, wildtype spindles have an in-between size and flux rate from spindles in Patronin depleted cells (higher flux/shorter spindles) and spindles in Klp10a depleted cells (lower flux/longer spindles), suggesting Klp10a's access to free minus ends governs metaphase spindle size. Similarly, GFP-Patronin localizes to a subset of microtubules in interphase, but appears diffuse throughout the metaphase spindle, resuming its selective localization at the end of anaphase. This suggests some kind of cell-cycle controlled regulatory event. Whether this is a post-translational modification on Patronin, loss of an interaction partner in mitosis, or degradation of the protein remains to be determined.

Non-centrosomal microtubule arrays and γ-TuRC

How non-centrosomal microtubule arrays, or microtubule arrays that are not radially organized around a centrosome, are formed is still unknown. Pieces of this puzzle have been put together through studies of different cell types, such as neurons,

epithelial cells, and cells in flies, plants, and fungi. It seems that generally microtubules are nucleated from a main site, like the centrosome, or from multiple sites throughout the cell by an unknown combination of proteins. Microtubules are then released from this nucleating material and somehow transported to specific sites throughout the cell. Since non-centrosomal microtubule arrays form a variety of shapes and sizes, these last two steps must be highly regulated. It is hypothesized that microtubule release may be a result of the activity of microtubule severing proteins or the lack of microtubule anchoring proteins at nucleation sites, however microtubule transport after release remains a mystery.

In plant cells, microtubules move by treadmilling, however in animal cells treadmilling is a rare phenomenon. Patronin may play an essential role in this step. In Drosophila, lack of Patronin results in microtubules treadmilling away from sites of nucleation. Therefore in wildtype cells, Patronin presumably binds to and stabilizes minus ends shortly after nucleation. Indeed, Patronin's interactions with Sas-4 and SAK would place it near sites of new microtubule nucleation. It is hypothesized that in non-centrosomal arrays, microtubules are transported by motor proteins and anchored to specific sites throughout the cell by unknown proteins. In order for the microtubule to be transported, the minus end must be stabilized. Patronin could serve both as a minus end stabilizer and as the link between the microtubule and sites throughout the cell by binding to the minus end shortly after it is released from nucleation centers and transporting with it to discrete locations in the cytoplasm. This may be occurring in epithelial cells, where microtubules originate from a centrosome, travel across the cell, and anchor to specific

sites in the apical region. Supporting this hypothesis, the human Patronin 3 homolog, Nezha, is found at such apical sites at the minus ends of microtubules (Meng et al., 2008). Something similar may be occurring in neurons, where centrosomes are not needed for axon growth or regeneration (Stiess et al., 2010). In the absence of centrosomes, microtubules nucleate throughout the cell and organize to regenerate axons or promote axon growth suggesting the nucleation, stabilization, and organization of microtubules by yet to be identified proteins.

Another question is whether Patronin interacts or overlaps in function with γ-tubulin. The importance of γ-tubulin in non-centrosomal microtubule arrays remains to be determined. Although γ-tubulin is the only microtubule nucleator known to date, Drosophila can still re-generate microtubules in γ-tubulin depleted cells in colcemid regrowth experiments (Rogers et al., 2008) and RNAi of γ-TuRC components does not affect microtubule organization in interphase (Bouissou et al., 2009). As purified Patronin selectively binds to minus ends of microtubules made of purified tubulin, it is likely that Patronin and γ-tubulin have separate functions.

In sum, the identification of a minus end capping protein opens up the door to new areas of research and is a major step in identifying the minus end regulatory network. The studies described in this thesis also further our understanding of how cells are able to create such diverse organizations of the microtubule cytoskeleton.

References

Akhmanova, A., and Steinmetz, M. (2008). Tracking the ends: a dynamic protein network controls the fate of microtubule tips. Nat Rev Mol Cell Biol *9*, 309-22.

Baines, A. J., Bignone, P. A., King, M. D., Maggs, A. M., Bennett, P. M., Pinder, J. C., and Phillips, G. W. (2009). The CKK domain (DUF1781) domain binds microtubules and defines the CAMSAP/ssp4 family of animal proteins. Mol Biol Evol *26*, 2005-14.

Bartolini, F., and Gundersen, G. G. (2006). Generation of noncentrosomal microtubule arrays. J Cell Sci *119*, 4155-63.

Berglund, L., Björling, E., Oksvold, P., Fagerberg, L., Asplund, A., Al-Khalili Szigyarto, C., Persson, A., Ottosson, J., Wernérus, H., Nilsson, P., et al. (2008). A genecentric Human Protein Atlas for expression profiles based on antibodies. Mol Cell Proteomics *7*, 2019-27.

Bettencourt-Dias, M., and Glover, D. M. (2007). Centrosome biogenesis and function: centrosomics brings new understanding. Nat Rev Mol Cell Biol *8*, 451-63.

Bouissou, A., Vérollet, C., Sousa, A., Sampaio, P., Wright, M., Sunkel, C. E., Merdes, A., and Raynaud-Messina, B. (2009). {gamma}-Tubulin ring complexes regulate microtubule plus end dynamics. J Cell Biol *187*, 327-34.

van Breugel, M., Hirono, M., Andreeva, A., Yanagisawa, H.-A., Yamaguchi, S., Nakazawa, Y., Morgner, N., Petrovich, M., Ebong, I.-O., Robinson, C. V., et al.

(2011). Structures of SAS-6 Suggest Its Organization in Centrioles. Science. *331,* 1196-9.

Cizmecioglu, O., Arnold, M., Bahtz, R., Settele, F., Ehret, L., Haselmann-Weiss, U., Antony, C., and Hoffmann, I. (2010). Cep152 acts as a scaffold for recruitment of Plk4 and CPAP to the centrosome. J Cell Biol *191*, 731-739.

Cooper, J. R., Wagenbach, M., Asbury, C. L., and Wordeman, L. (2009). Catalysis of the microtubule on-rate is the major parameter regulating the depolymerase activity of MCAK. Nature Structural & Molecular Biology *17*, 77-82.

Dammermann, A., Desai, A., and Oegema, K. (2003). The minus end in sight. Curr Biol *13*, R614-24.

Delgehyr, N., Sillibourne, J., and Bornens, M. (2005). Microtubule nucleation and anchoring at the centrosome are independent processes linked by ninein function. J Cell Sci *118*, 1565-75.

Desai, A., and Mitchison, T. J. (1997). Microtubule polymerization dynamics. Annu Rev Cell Dev Biol *13*, 83-117.

Desai, A., Verma, S., Mitchison, T. J., and Walczak, C. E. (1999). Kin I kinesins are microtubule-destabilizing enzymes. Cell *96*, 69-78.

Dumont, S., and Mitchison, T. J. (2009). Force and length in the mitotic spindle. Curr Biol *19*, R749-61.

Dzhindzhev, N. S., Yu, Q. D., Weiskopf, K., Tzolovsky, G., Cunha-Ferreira, I., Riparbelli, M., Rodrigues-Martins, A., Bettencourt-Dias, M., Callaini, G., and Glover, D. M. (2010). Asterless is a scaffold for the onset of centriole assembly. Nature *467*, 714-8.

Ehrhardt, D. W. (2008). Straighten up and fly right: microtubule dynamics and organization of non-centrosomal arrays in higher plants. Curr Opin Cell Biol *20*, 107-16.

Fan, J., Griffiths, A. D., Lockhart, A., Cross, R. A., and Amos, L. A. (1996). Microtubule minus ends can be labelled with a phage display antibody specific to alpha-tubulin. J Mol Biol *259*, 325-30.

Goshima, G., and Vale, R. D. (2005). Cell cycle-dependent dynamics and regulation of mitotic kinesins in Drosophila S2 cells. Mol Biol Cell *16*, 3896-907.

Goshima, G., and Vale, R. D. (2003). The roles of microtubule-based motor proteins in mitosis: comprehensive RNAi analysis in the Drosophila S2 cell line. J Cell Biol *162*, 1003-16.

Goshima, G., Wollman, R., Goodwin, S. S., Zhang, N., Scholey, J. M., Vale, R. D., and Stuurman, N. (2007). Genes required for mitotic spindle assembly in Drosophila S2 cells. Science *316*, 417-21.

Goshima, G., Wollman, R., Stuurman, N., Scholey, J. M., and Vale, R. D. (2005). Length control of the metaphase spindle. Curr Biol *15*, 1979-88.

Hatch, E. M., Kulukian, A., Holland, A. J., Cleveland, D. W., and Stearns, T. (2010). Cep152 interacts with Plk4 and is required for centriole duplication. J Cell Biol *191*, 721-729.

Howard, J., and Hyman, A. A. (2007). Microtubule polymerases and depolymerases. Curr Opin Cell Biol *19*, 31-5.

Hughes, J. R., Meireles, A. M., Fisher, K. H., Garcia, A., Antrobus, P. R., Wainman, A., Zitzmann, N., Deane, C., Ohkura, H., Wakefield, J. G., et al. (2008). A Microtubule Interactome: Complexes with Roles in Cell Cycle and Mitosis. Plos Biol *6*, e98.

Hunter, A. W., Caplow, M., Coy, D. L., Hancock, W. O., Diez, S., Wordeman, L., and Howard, J. (2003). The kinesin-related protein MCAK is a microtubule depolymerase that forms an ATP-hydrolyzing complex at microtubule ends. Mol Cell *11*, 445-57.

Keating, T. J., Peloquin, J. G., Rodionov, V. I., Momcilovic, D., and Borisy, G. G. (1997). Microtubule release from the centrosome. Proc Natl Acad Sci USA *94*, 5078-83.

Kinoshita, K., Arnal, I., Desai, A., Drechsel, D. N., and Hyman, A. A. (2001). Reconstitution of physiological microtubule dynamics using purified components. Science *294*, 1340-3.

Kirkham, M., Muller-Reichert, T., Oegema, K., Grill, S., and Hyman, A. (2003). SAS-4 is a C. elegans centriolar protein that controls centrosome size. Cell *112*, 575-87.

Kitagawa, D., Vakonakis, I., Olieric, N., Hilbert, M., Keller, D., Olieric, V., Bortfeld, M., Erat, M. C., Flückiger, I., Gönczy, P., et al. (2011). Structural basis of the 9-fold symmetry of centrioles. Cell *144*, 364-375.

Kner, P., Chhun, B. B., Griffis, E. R., Winoto, L., and Gustafsson, M. G. (2009). Super-resolution video microscopy of live cells by structured illumination. Nat Meth *6*, 339-42.

Kwok, B. H., and Kapoor, T. M. (2007). Microtubule flux: drivers wanted. Curr Opin Cell Biol *19*, 36-42.

Lansbergen, G., and Akhmanova, A. (2006). Microtubule plus end: a hub of cellular activities. Traffic *7*, 499-507.

Laycock, J. E., Savoian, M. S., and Glover, D. M. (2006). Antagonistic activities of Klp10A and Orbit regulate spindle length, bipolarity and function in vivo. J Cell Sci *119*, 2354-61.

Li, K., and Kaufman, T. (1996). The homeotic target gene centrosomin encodes an essential centrosomal component. Cell *85*, 585-96.

Lupas, A., Van Dyke, M., and Stock, J. (1991). Predicting Coiled Coils from Protein Sequences. Science *252*, 1162-1164.

Mahoney, N. M., Goshima, G., Douglass, A. D., and Vale, R. D. (2006). Making microtubules and mitotic spindles in cells without functional centrosomes. Curr Biol *16*, 564-9.

Meng, W., Mushika, Y., Ichii, T., and Takeichi, M. (2008). Anchorage of microtubule minus ends to adherens junctions regulates epithelial cell-cell contacts. Cell *135*, 948-59.

Mennella, V., Rogers, G. C., Rogers, S. L., Buster, D. W., Vale, R. D., and Sharp, D. J. (2005). Functionally distinct kinesin-13 family members cooperate to regulate microtubule dynamics during interphase. Nat Cell Biol *7*, 235-45.

Mitchison, T., and Kirschner, M. (1984). Dynamic instability of microtubule growth. Nature *312*, 237-42.

Mitchison, T. J. (1993). Localization of an exchangeable GTP binding site at the plus end of microtubules. Science *261*, 1044-7.

Mitchison, T. J., Maddox, P., Gaetz, J., Groen, A., Shirasu, M., Desai, A., Salmon, E. D., and Kapoor, T. M. (2005). Roles of polymerization dynamics, opposed motors, and a tensile element in governing the length of Xenopus extract meiotic spindles. Mol Biol Cell *16*, 3064-76.

Moores, C. A., and Milligan, R. A. (2006). Lucky 13-microtubule depolymerisation by kinesin-13 motors. J Cell Sci *119*, 3905-13.

Moores, C. A., Yu, M., Guo, J., Beraud, C., Sakowicz, R., and Milligan, R. A. (2002). A mechanism for microtubule depolymerization by KinI kinesins. Mol Cell *9*, 903-9.

Moritz, M., and Agard, D. A. (2001). Gamma-tubulin complexes and microtubule nucleation. Curr Opin Struct Biol *11*, 174-81.

Moritz, M., Braunfeld, M., Sedat, J., Alberts, B., and Agard, D. (1995). Microtubule nucleation by gamma-tubulin-containing rings in the centrosome. Nature *378*, 638-40.

Nogales, E., and Wang, H. W. (2006). Structural intermediates in microtubule assembly and disassembly: how and why? Curr Opin Cell Biol *18*, 179-84.

O'Connell, K. F., Caron, C., Kopish, K. R., Hurd, D. D., Kemphues, K. J., Li, Y., and White, J. G. (2001). The C. elegans zyg-1 gene encodes a regulator of centrosome duplication with distinct maternal and paternal roles in the embryo. Cell *105*, 547-558.

Peel, N., Stevens, N., Basto, R., and Raff, J. (2007). Overexpressing centriole-replication proteins in vivo induces centriole overduplication and de novo formation. Curr Biol *17*, 834-43.

Rath, U., Rogers, G. C., Tan, D., Gomez-Ferreria, M. A., Buster, D. W., Sosa, H. J., and Sharp, D. J. (2009). The Drosophila Kinesin-13, KLP59D, Impacts Pacman and Flux-based Chromosome Movement. Mol Biol Cell. *20,* 4696-705.

Reck-Peterson, S. L., Yildiz, A., Carter, A. P., Gennerich, A., Zhang, N., and Vale, R. D. (2006). Single-molecule analysis of dynein processivity and stepping behavior. Cell *126*, 335-48.

Rodionov, V., Nadezhdina, E., and Borisy, G. (1999). Centrosomal control of microtubule dynamics. Proc Natl Acad Sci USA *96*, 115-20.

Rodionov, V. I., and Borisy, G. G. (1997). Microtubule treadmilling in vivo. Science *275*, 215-8.

Rogers, G. C., Rogers, S. L., Schwimmer, T. A., Ems-McClung, S. C., Walczak, C. E., Vale, R. D., Scholey, J. M., and Sharp, D. J. (2004). Two mitotic kinesins cooperate to drive sister chromatid separation during anaphase. Nature *427*, 364-70.

Rogers, G. C., Rusan, N. M., Peifer, M., and Rogers, S. L. (2008). A multicomponent assembly pathway contributes to the formation of acentrosomal microtubule arrays in interphase Drosophila cells. Mol Biol Cell *19*, 3163-78.

Rogers, S. L., Rogers, G. C., Sharp, D. J., and Vale, R. D. (2002). Drosophila EB1 is important for proper assembly, dynamics, and positioning of the mitotic spindle. J Cell Biol *158*, 873-84.

Rogers, S. L., Wiedemann, U., Stuurman, N., and Vale, R. D. (2003). Molecular requirements for actin-based lamella formation in Drosophila S2 cells. J Cell Biol *162*, 1079-88.

Rusan, N. M., and Rogers, G. C. (2009). Centrosome Function: Sometimes Less Is More. Traffic *10*, 472-81.

Shaw, S. L., Kamyar, R., and Ehrhardt, D. W. (2003). Sustained microtubule treadmilling in Arabidopsis cortical arrays. Science *300*, 1715-8.

Stiess, M., Maghelli, N., Kapitein, L. C., Gomis-Rüth, S., Wilsch-Bräuninger, M., Hoogenraad, C. C., Tolić-Nørrelykke, I. M., and Bradke, F. (2010). Axon extension occurs independently of centrosomal microtubule nucleation. Science *327*, 704-7.

Stuurman, N., Amodaj, N., and Vale, R. D. (2007). Micro-Manager: Open Source software for light microscope imaging. Microscopy Today *15*, 42-43.

Varmark, H., Llamazares, S., Rebollo, E., Lange, B., Reina, J., Schwarz, H., and Gonzalez, C. (2007). Asterless is a centriolar protein required for centrosome function and embryo development in Drosophila. Curr Biol *17*, 1735-45.

Vérollet, C., Colombié, N., Daubon, T., Bourbon, H. M., Wright, M., and Raynaud-Messina, B. (2006). Drosophila melanogaster gamma-TuRC is dispensable for targeting gamma-tubulin to the centrosome and microtubule nucleation. J Cell Biol *172*, 517-28.

Vorobjev, I. A., Rodionov, V. I., Maly, I. V., and Borisy, G. G. (1999). Contribution of plus and minus end pathways to microtubule turnover. J Cell Sci *112 (Pt 14)*, 2277-89.

Vorobjev, I., Svitkina, T., and Borisy, G. (1997). Cytoplasmic assembly of microtubules in cultured cells. J Cell Sci *110 (Pt 21)*, 2635-45.

Waterman-Storer, C., and Salmon, E. (1997). Actomyosin-based retrograde flow of microtubules in the lamella of migrating epithelial cells influences microtubule dynamic instability and turnover and is associated with microtubule breakage and treadmilling. J Cell Biol *139*, 417-34.

Wiese, C., and Zheng, Y. (2000). A new function for the gamma-tubulin ring complex as a microtubule minus-end cap. Nat Cell Biol *2*, 358-64.

Woehlke, G., Ruby, A. K., Hart, C. L., Ly, B., Hom-Booher, N., and Vale, R. D. (1997). Microtubule interaction site of the kinesin motor. Cell *90*, 207-16.

Yamamoto, M., Yoshimura, K., Kitada, M., Nakahara, J., Seiwa, C., Ueki, T., Shimoda, Y., Ishige, A., Watanabe, K., and Asou, H. (2009). A new monoclonal antibody, A3B10, specific for astrocyte-lineage cells recognizes calmodulin-regulated spectrin-associated protein 1 (Camsap1). J Neurosci Res *87*, 503-13.

Yvon, A. M., and Wadsworth, P. (1997). Non-centrosomal microtubule formation and measurement of minus end microtubule dynamics in A498 cells. J Cell Sci *110 (Pt 19)*, 2391-401.

Zheng, Y., Wong, M., Alberts, B., and Mitchison, T. (1995). Nucleation of microtubule assembly by a gamma-tubulin-containing ring complex. Nature *378*, 578-83.

Publishing Agreement

It is the policy of the University to encourage the distribution of all theses, dissertations, and manuscripts. Copies of all UCSF theses, dissertations, and manuscripts will be routed to the library via the Graduate Division. The library will make all theses, dissertations, and manuscripts accessible to the public and will preserve these to the best of their abilities, in perpetuity.

I hereby grant permission to the Graduate Division of the University of California, San Francisco to release copies of my thesis, dissertation, or manuscript to the Campus Library to provide access and preservation, in whole or in part, in perpetuity.

Sarah Goodwin 7/25/11

Author Signature Date